Applications of Dispersion-Corrected DFT to Molecular Crystals and Interfaces of Layered Materials

Erin R. Johnson
Department of Chemistry, Dalhousie University

Dispersion interactions

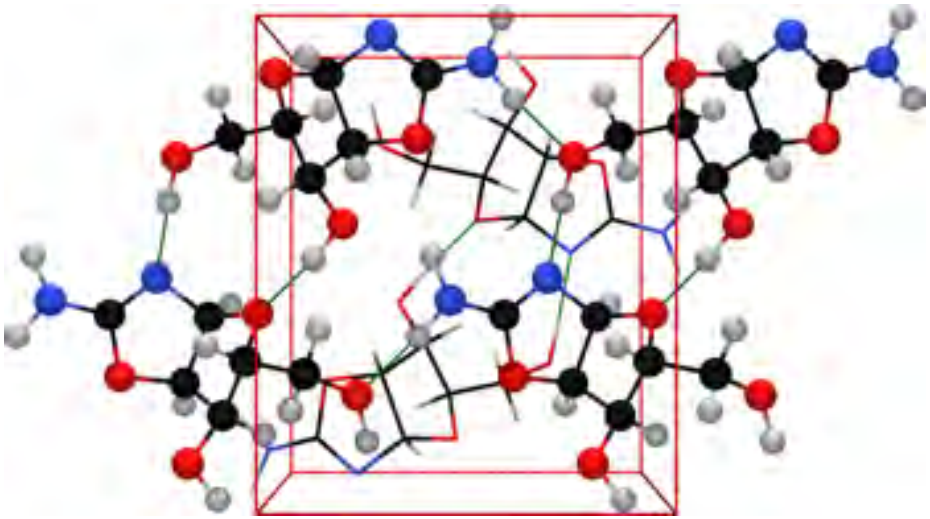

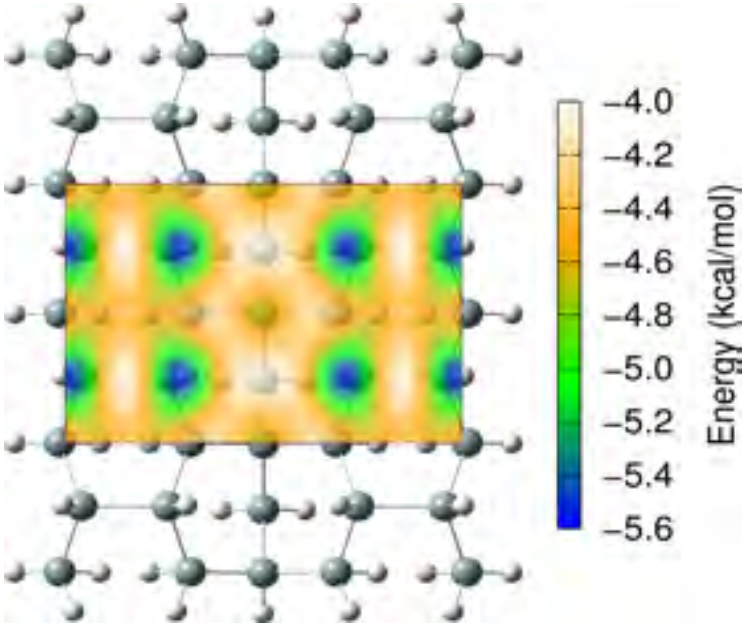

- Biomolecular structure
- Self-assembly
- Layered materials

- Surface adsorption
- Phase transitions
- Crystal packing

The XDM method

Dispersion arises from interaction of instantaneous dipoles.

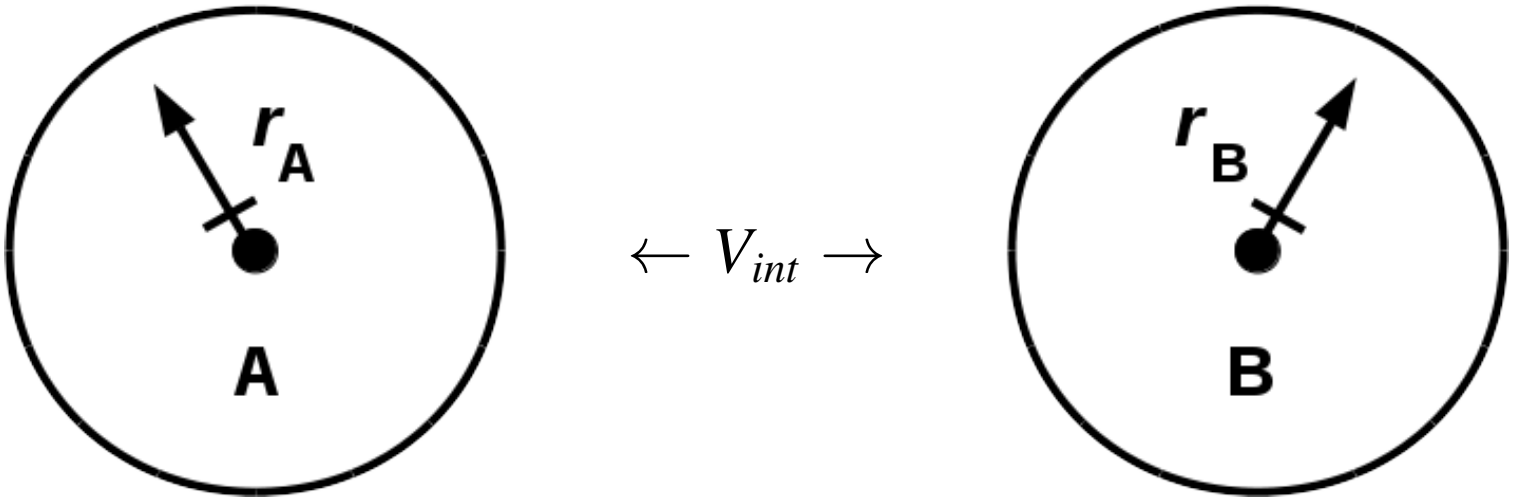

The source of the instantaneous dipole moments is taken to be the **dipole moment of the exchange(-correlation) hole**.

JCP **127** (2007) 154108

The exchange hole

The exchange hole measures the depletion in probability of finding another same-spin electron in the vicinity of a reference electron.

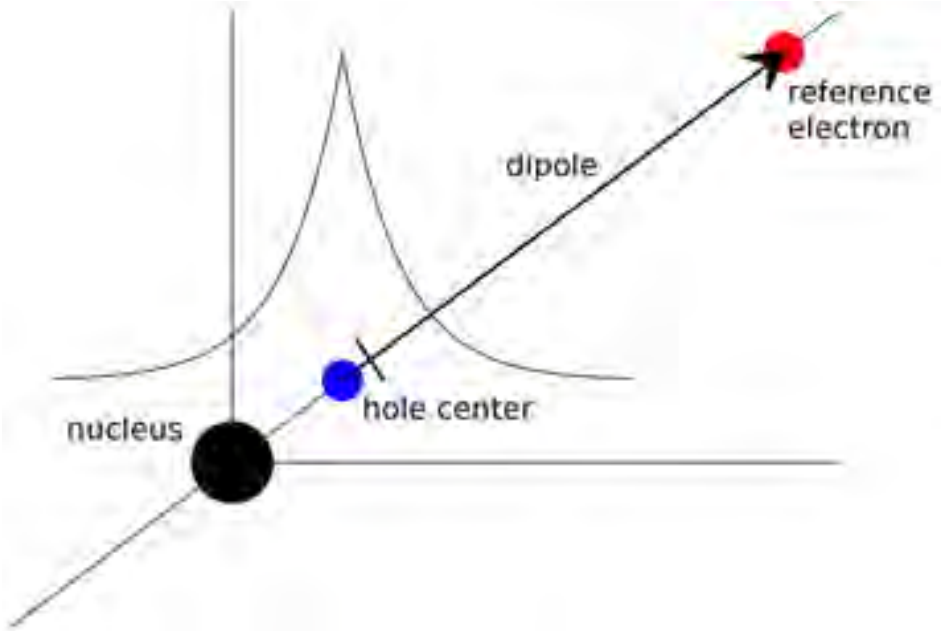

An electron plus its exchange hole has zero total charge, but a non-zero dipole moment in general.

The exchange-hole model

The magnitude d_X of the exchange-hole dipole moment is obtained using the Becke-Roussel exchange-hole model.

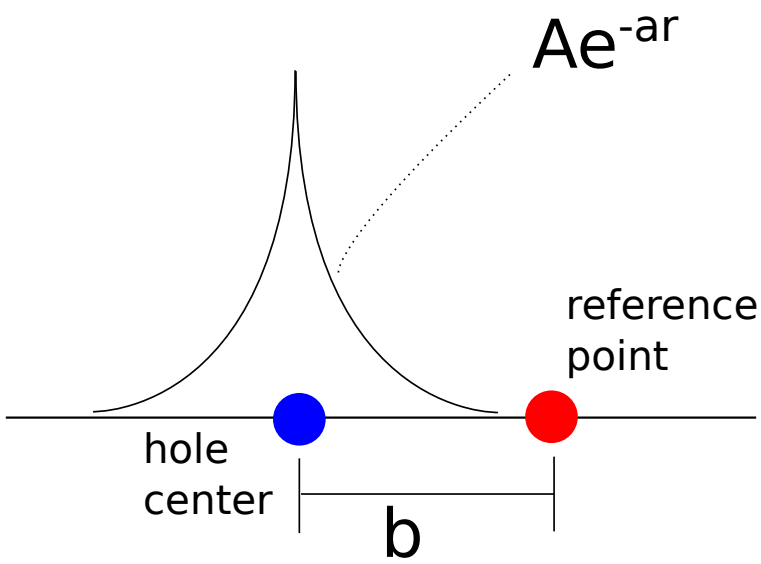

- Parameters (A,a,b) obtained from normalization, density, and curvature at reference point.
- Advantages: semi-local (meta-GGA) model of the dipole, $d_x = b$.

PRA **39** (1989) 3761

The XDM method

The dispersion energy comes from second-order perturbation theory

$$E^{(2)} = \frac{\langle \hat{V}_{int}^2 \rangle}{\Delta E}$$

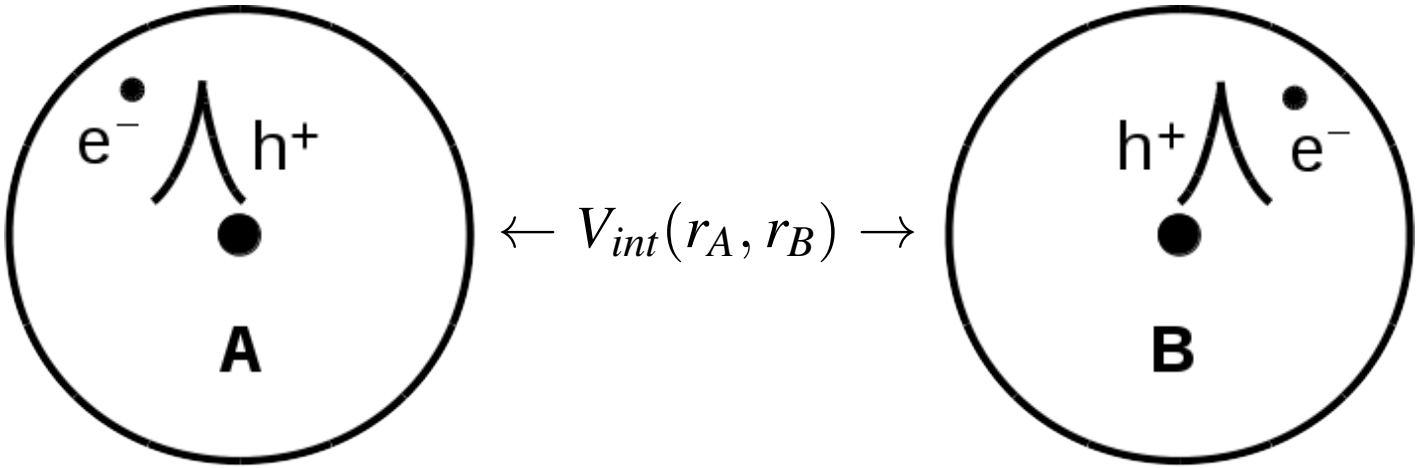

$V_{int}(r_A, r_B)$ = multipole moments of electron + hole at r_A interacting with multipole moments of electron + hole at r_B

ΔE is the average excitation energy, obtained from second-order pertubation theory applied to polarizability.

The XDM equations

The XDM dispersion energy is:

$$E_{disp} = -\frac{1}{2}\sum_{ij}\frac{C_6 f_6(R_{ij})}{R_{ij}^6} + \frac{C_8 f_8(R_{ij})}{R_{ij}^8} + \frac{C_{10} f_{10}(R_{ij})}{R_{ij}^{10}}$$

The dispersion coefficients are non-empirical:

$$C_{6,ij} = \frac{\alpha_i \alpha_j \langle M_1^2 \rangle_i \langle M_1^2 \rangle_j}{\alpha_i \langle M_1^2 \rangle_j + \alpha_j \langle M_1^2 \rangle_i}$$

The C_8 and C_{10} dispersion coefficients depend on higher-order multipole moments, M_l.

Damping function

Corrects for the multipolar-expansion error and avoids discontinuities.

$$f_n(R) = \frac{R^n}{R^n + R_{\text{vdw}}^n}$$

$$R_{\text{vdw}} = a_1 R_{c,ij} + a_2$$

$R_{c,ij}$ are proportional to atomic volumes and are determined from ratios of the dispersion coefficients.

a_1 and a_2 are parameters fit for use with a particular XC functional.

Implementation

Dispersion correction is added to base density-functional energies:

$$E = E_{DFT} + E_{disp}$$

Calculation of E_{disp} is fast compared to E_{DFT}.

XDM is implemented for use with

- **Gaussian** using **postg** (http://schooner.chem.dal.ca)
- **Quantum ESPRESSO**
- **SIESTA**
- **FHI-aims**

Benchmark set – KB49

49 gas-phase dimers

- dispersion
- π-stacking
- dipole - induced dipole
- mixed
- dipole - dipole
- hydrogen-bonding

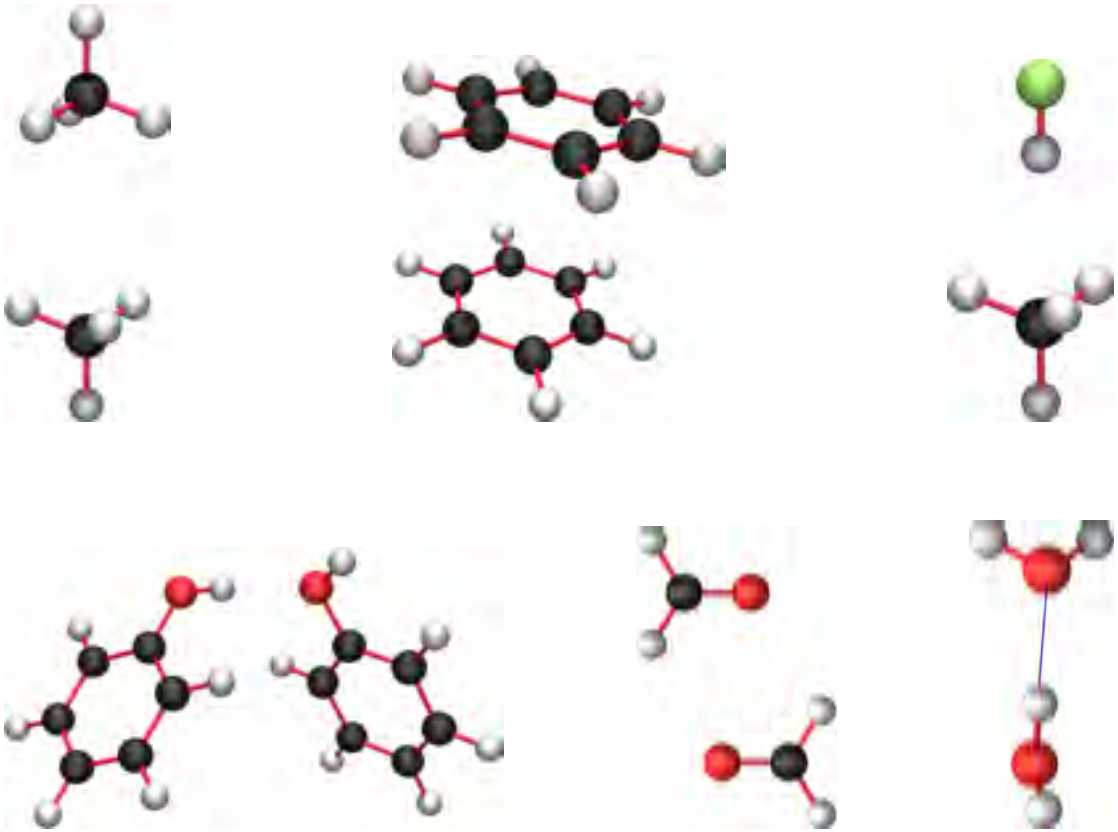

Dispersionless base functionals

The base density functional should be dispersionless and give an accurate treatment of non-bonded repulsion.

Mean absolute errors, in kcal/mol, for the KB49 set and the X23 lattice-energy benchmark:

Functional	*KB49*	*X23*
PBEsol	*0.78*	*2.11*
PW91	*0.63*	*1.89*
PBE	*0.50*	*1.11*
PW86PBE	*0.41*	*0.88*
B86bPBE	*0.41*	*0.85*

B86b is our preferred exchange GGA to pair with XDM dispersion.

Importance of higher-order terms

Mean (absolute) errors, in kcal/mol, with B86bPBE-XDM:

Pairwise Terms			*Molecules – KB49*		*Crystals – X23*	
C_6	C_8	C_{10}	*MAE*	*ME*	*MAE*	*ME*
×			*0.83*	*-0.23*	*1.97*	*-1.59*
×	×		*0.48*	*0.02*	*0.94*	*-0.38*
×	×	×	*0.41*	*0.03*	*0.85*	*-0.26*

Inclusion of C_8 is essential for good performance for π-stacks and for molecular crystals.

PCCP **22**, 8266 (2020)

Graphite exfoliation

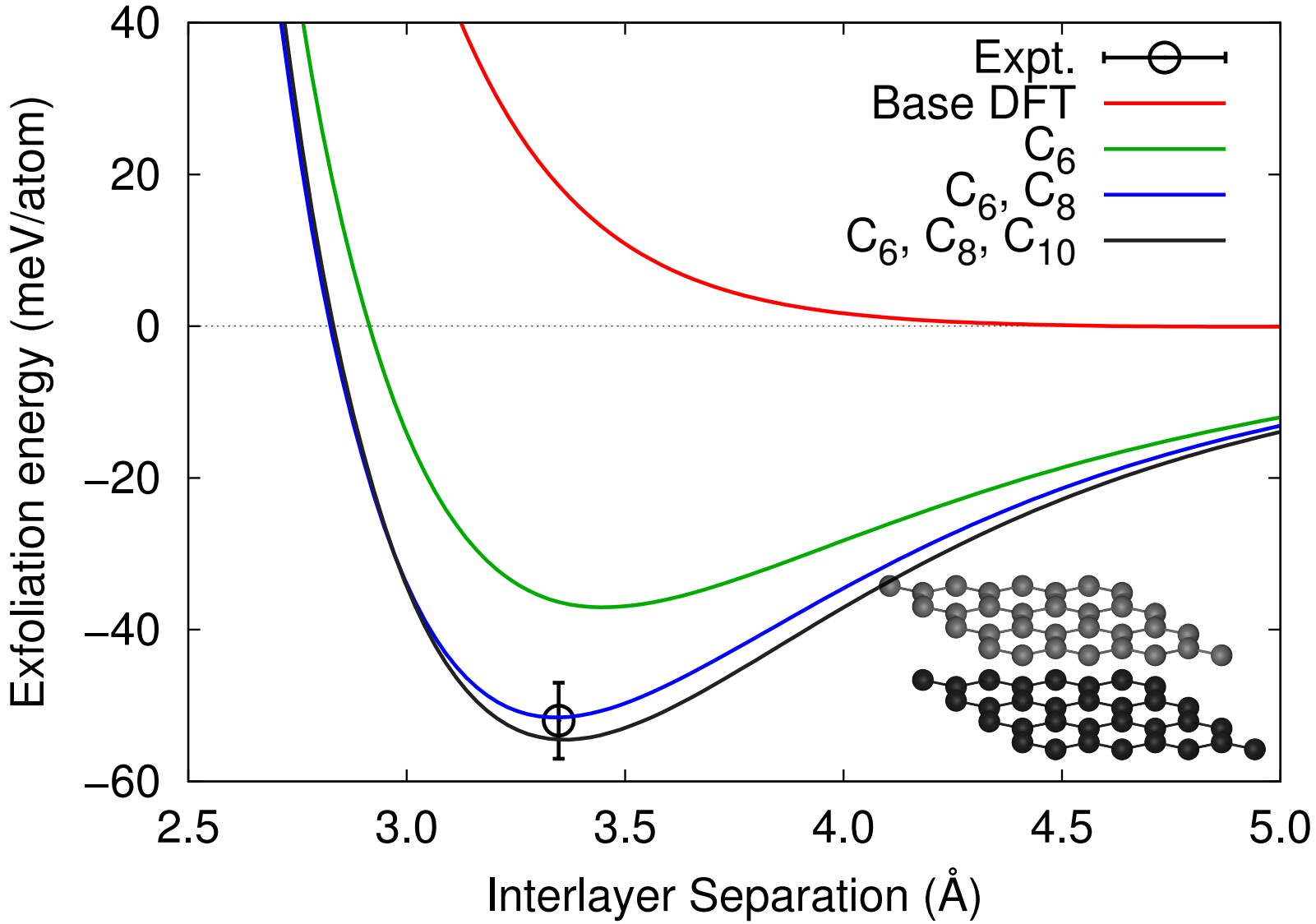

Layered materials

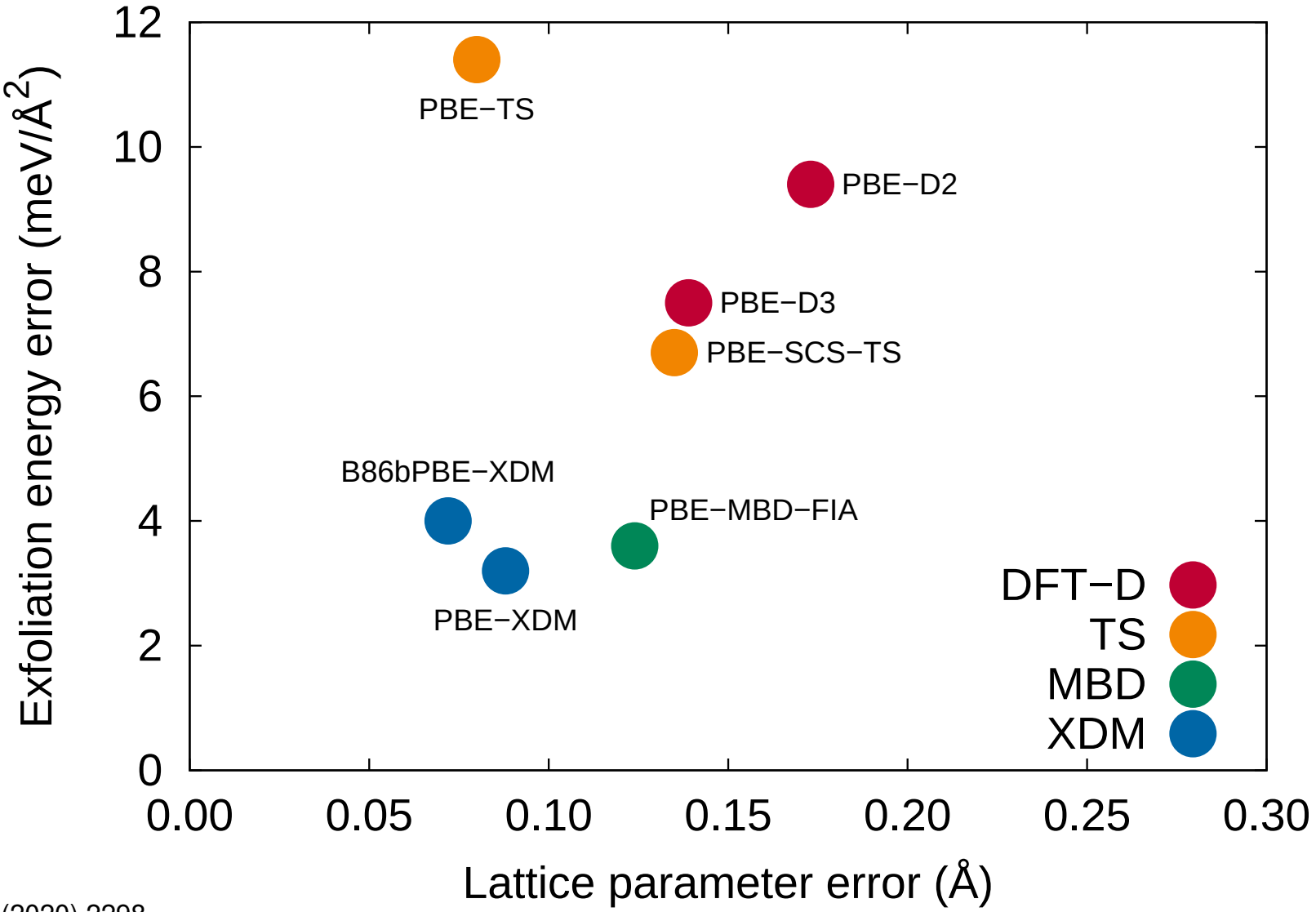

JPCL **11** (2020) 2298

Benzene adsorption on noble metals

Mean absolute errors (kcal/mol) relative to TPD reference data:

Method	*MAE*
PBE-D2	*10.0*
PBE-TS	*5.8*
PBE-D3	*4.4*
vdW-DF2	*3.5*
PBE-XDM	*2.2*
PBE-MBD	*1.8*
B86bPBE-XDM	*0.8*

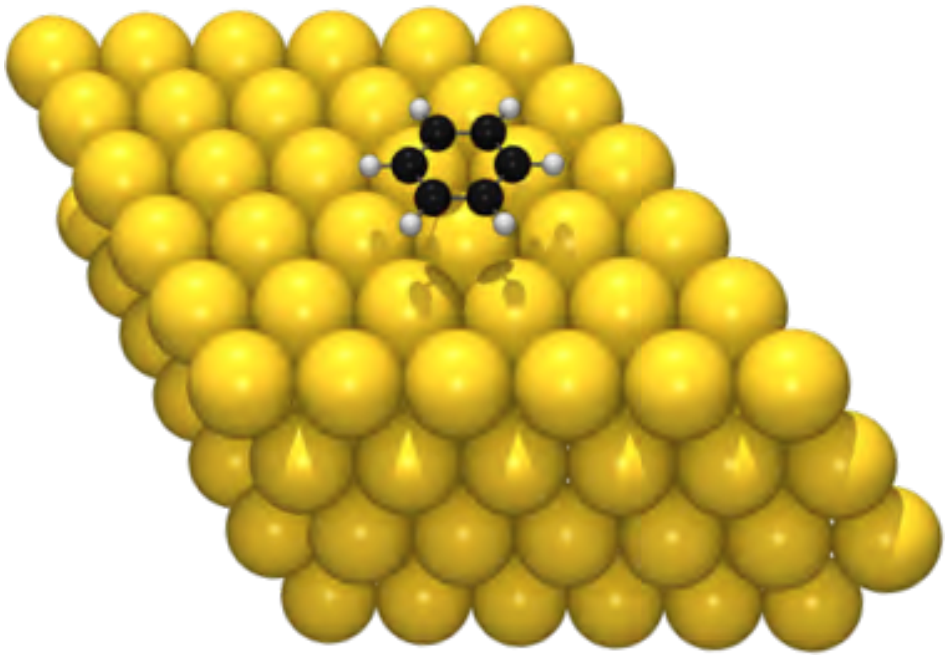

JCTC **12** (2016) 3305

Crystal-structure prediction (CSP)

First-principles CSP is a grand challenge in chemistry.

Crystal polymorphs have different:

- packing arrangements
- electronic energies
- sublimation energies
- melting points
- solubilities
- bio-availability
- charge transport

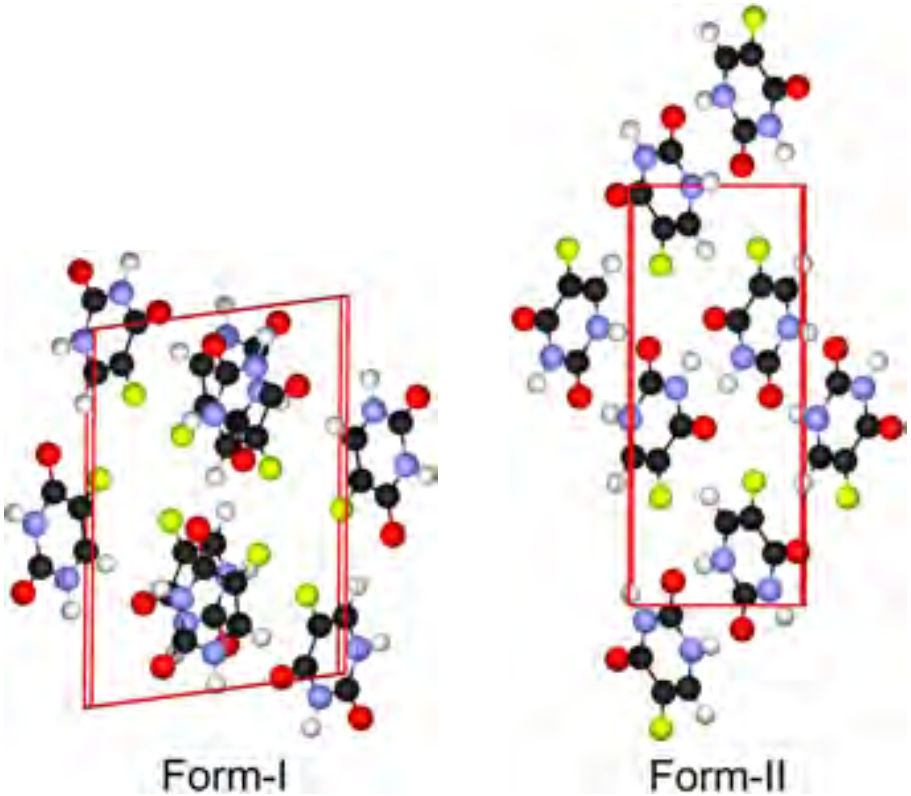

CSP requires extensive structure generation and accurate energy ranking.

CSP blind tests

The Cambridge Crystallographic Data Centre announces a set of compounds with known, but unpublished, crystal structures.

Computational predictions are compared to experimental x-ray structures.

Consider the submissions to the first 5 blind tests as a benchmark set.

Assess whether B86bPBE-XDM can predict the experimental structure as lowest in energy.

JCTC **13**, 441 and 5332 (2017)

Rigid, near-planar molecules

Molecule	*DFT-XDM*	*Molecule*	*DFT-XDM*
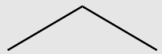	✓	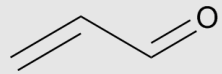	✓
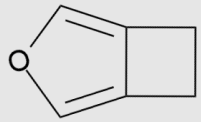	✓	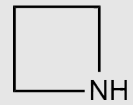	✓
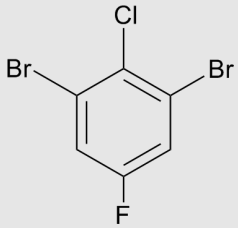	✓	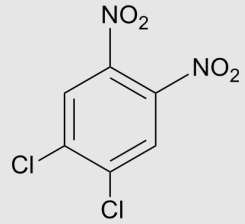	✓
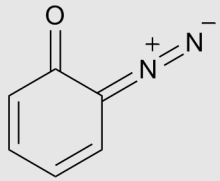	✓	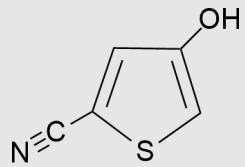	✗
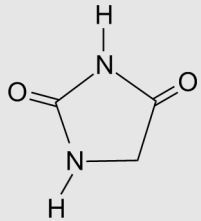	✓	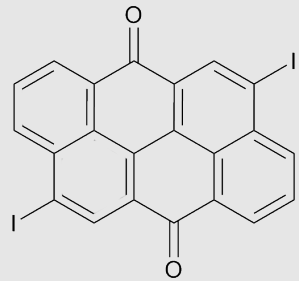	✓

Flexible or non-planar molecules and co-crystals

Molecule	*DFT-XDM*	*Molecule*	*DFT-XDM*
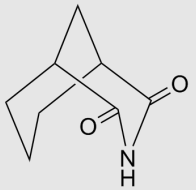	✓	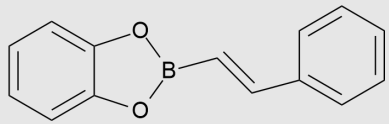	✓
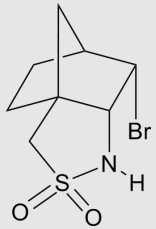	✗	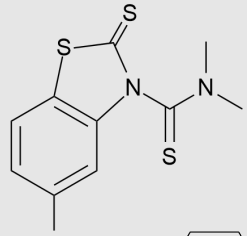	✓
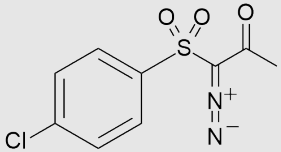	✓	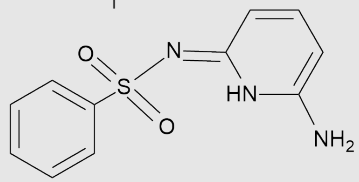	✓
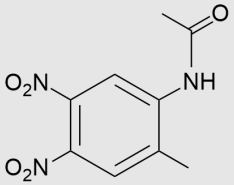	✗	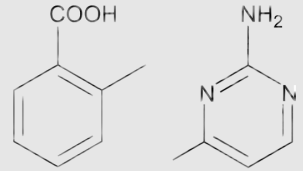	✓
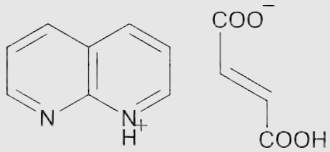	✗	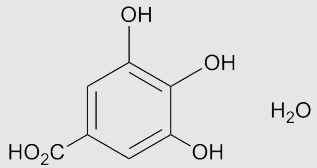	✓

Outliers: Delocalization and thermal vibrations

B86bPBE-XDM obtains the correct ranking in 16/20 cases.

Free-energy corrections for thermal vibrations are needed to recover the correct ranking for:

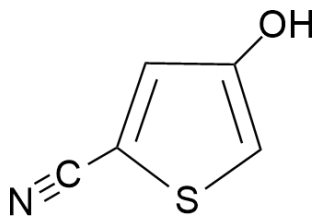

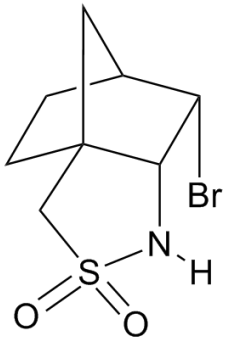

Delocalization error in the base functional is responsible for incorrect ranking in:

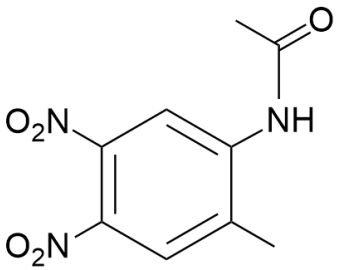

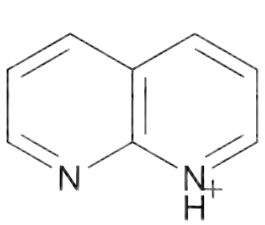

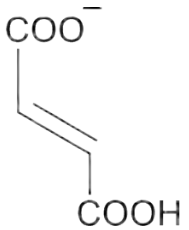

JCTC **13**, 441 and 5332 (2017)

5-Fluorouracil

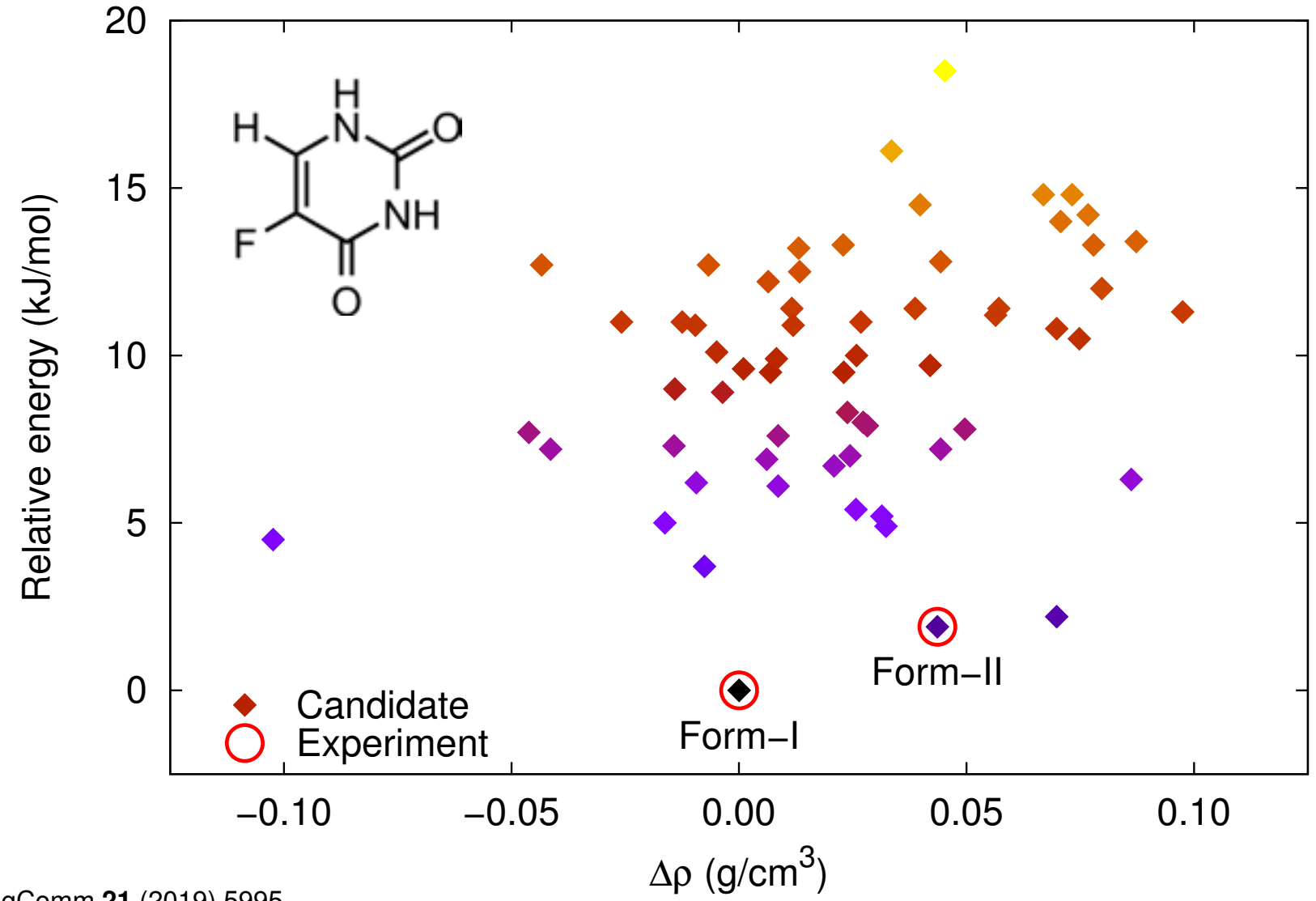

CrystEngComm **21** (2019) 5995

Olanzapine

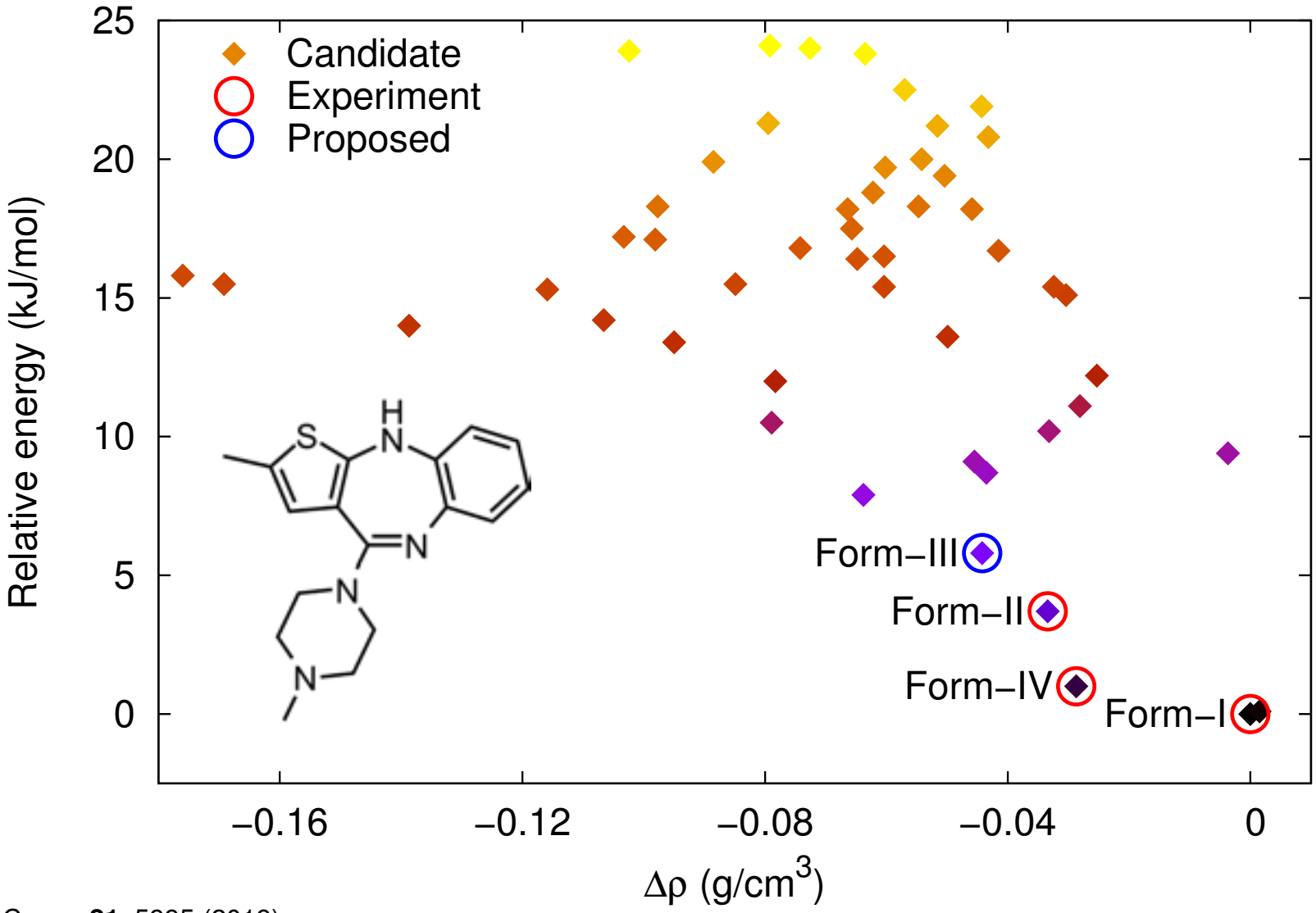

CrystEngComm **21**, 5995 (2019)

CSP of 1-aza[6]helicene

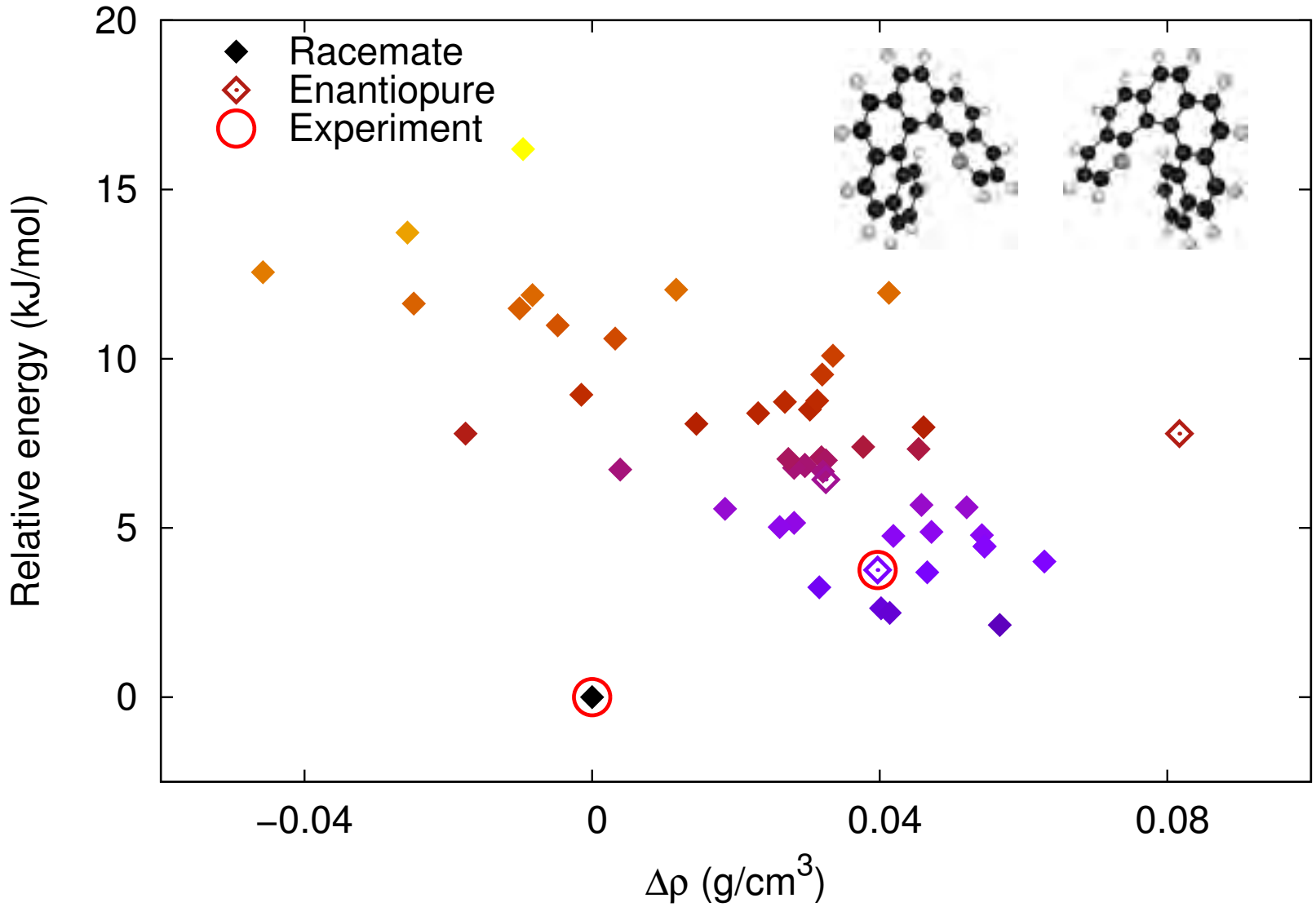

ACS Nano, **11** (2017) 8329

Crystal engineering of properties

Properties of a material are due a combination of the single molecule and the intermolecular interactions within the bulk.

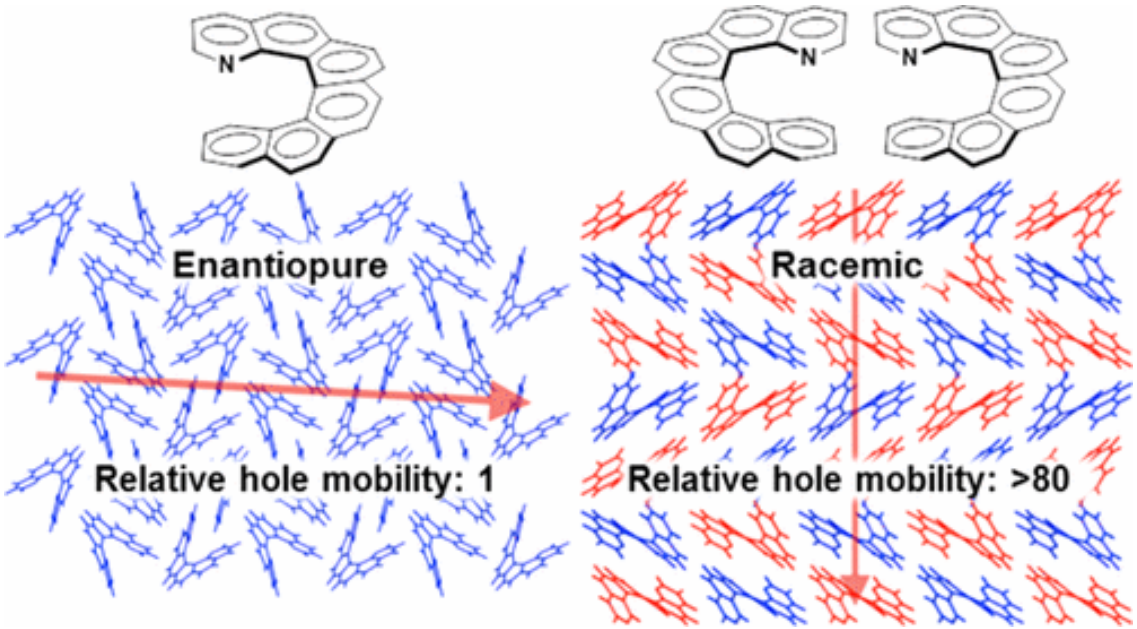

Screen substituted helicenes to target those that form polymorphs with high charge mobilities.

Screening substituted helicenes

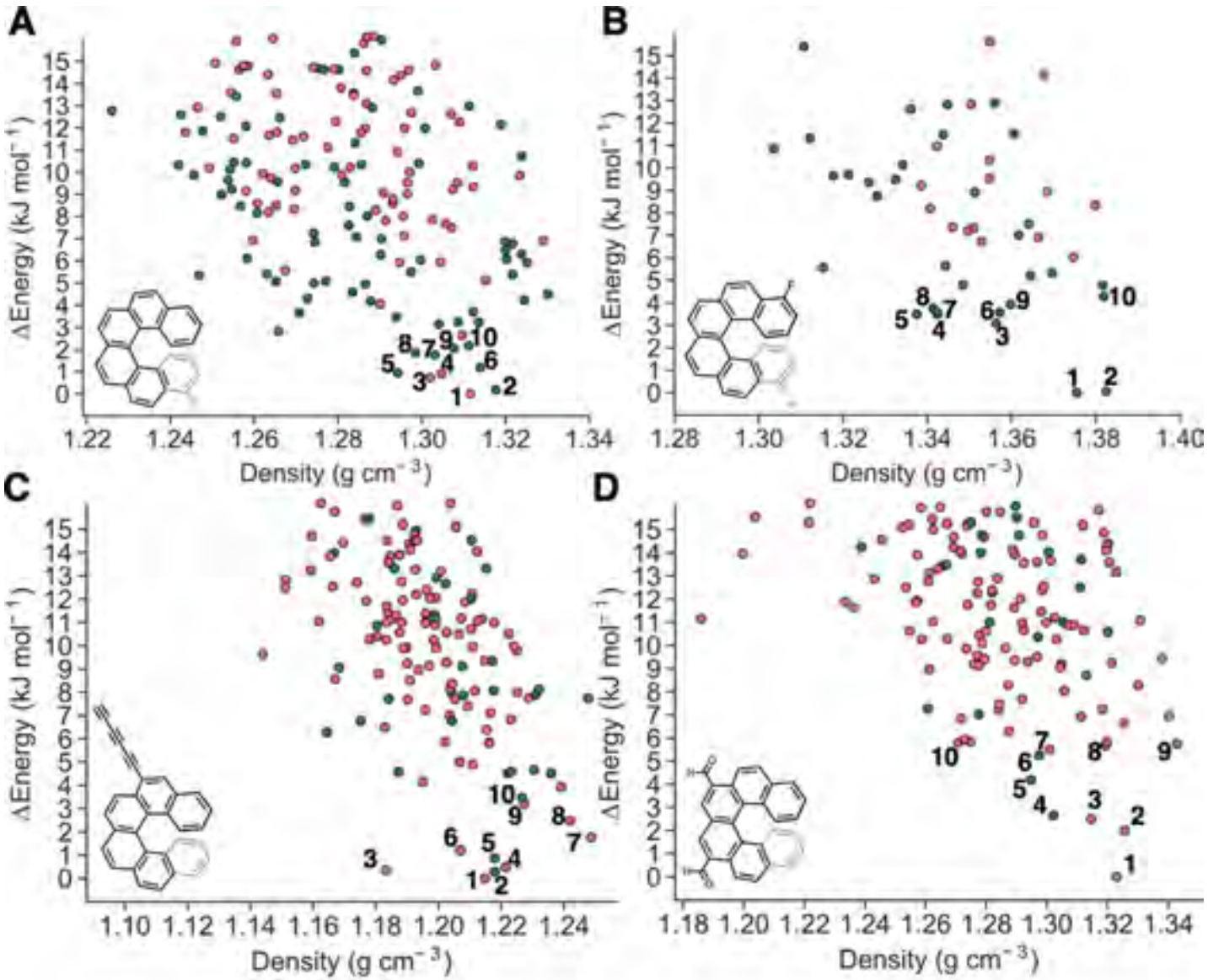

Predicted electron mobilities

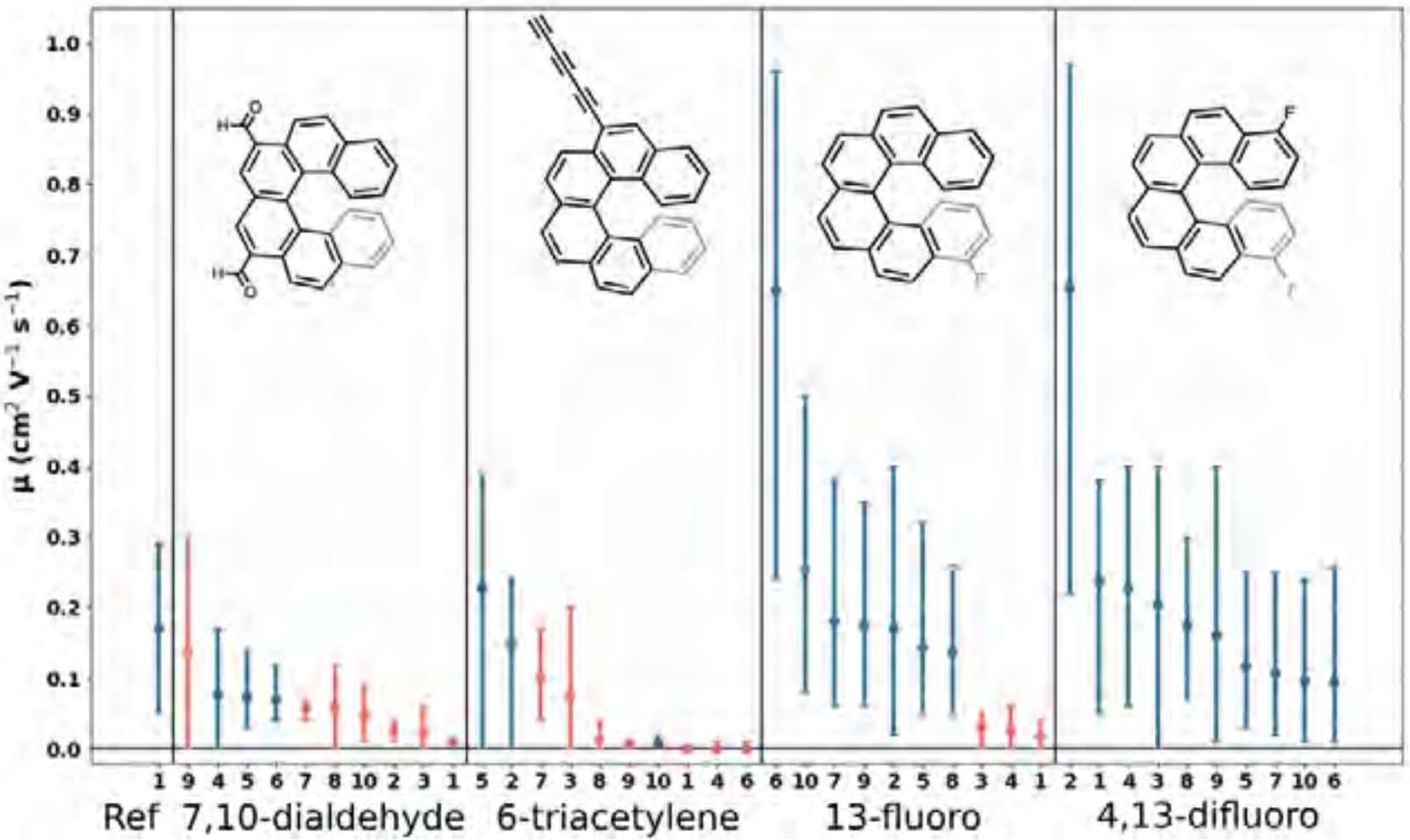

Cryst. Growth Des., **21** (2021) 5036

Numerical Atom-centred Orbitals (NAOs)

NAOs allow all-electron modeling of molecules and solids, with roughly linear scaling.

The radial components are numerical solutions to the Schrödinger-like equation:

$$\left(-\frac{1}{2}\frac{d^2}{dr^2}+\frac{\ell(\ell+1)}{r^2}+v_i(r)+v_{\text{cut}}(r)\right)u_i(r)=\varepsilon_i u_i(r).$$

The potential, $v_i(r)=Z_{\text{eff}}/r$, reflects orbital size and $v_{\text{cut}}(r)$ causes $u_i(r)$ to decay to zero beyond some cutoff radius.

NAO-DFT for molecular crystals

MAEs for sublimation enthalpies (in kcal/mol) of the X23 set of molecular crystals using NAOs:

FHI-aims
The ab initio materials simulation package

Functional	*Light*	*Tight*
PBE-TS	*4.17*	*3.14*
PBE-MBD	*1.61*	*0.94*
PBE-XDM	*1.14*	*1.04*
B86bPBE-XDM	*0.83*	*0.72*
PBE0-MBD	*1.97*	*1.07*
PBE0-XDM	*1.01*	*0.96*
B86bPBE-25X-XDM	***0.69***	***0.48***
B86bPBE-50X-XDM	*0.70*	*0.53*

Compound X from the 3rd CSP Blind Test

Delocalization error favours extended conjugation, rather than intermolecular H-bonding.

A MP2 monomer energy correction improves the B86bPBE-XDM energy ranking:

Structure	ΔE_{DFT}	$\Delta E_{\text{DFT+MP2}}$
Experiment	0.00	0.00
GGA minimum	-0.44	0.24

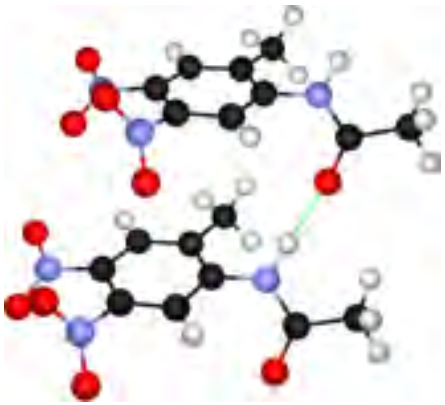

Experiment

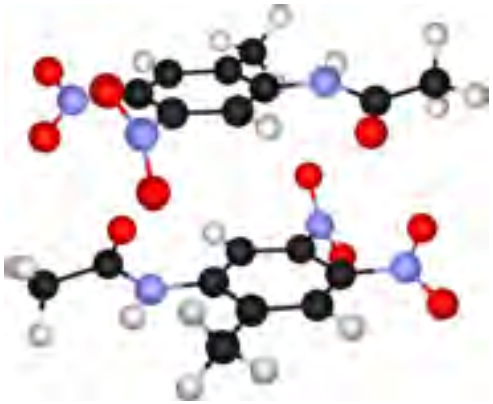

GGA minimum

JCTC **13** (2017) 5332

Compound X from the 3rd CSP Blind Test

Inclusion of exact exchange reverses the energy ranking.

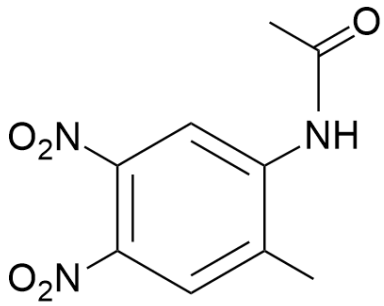

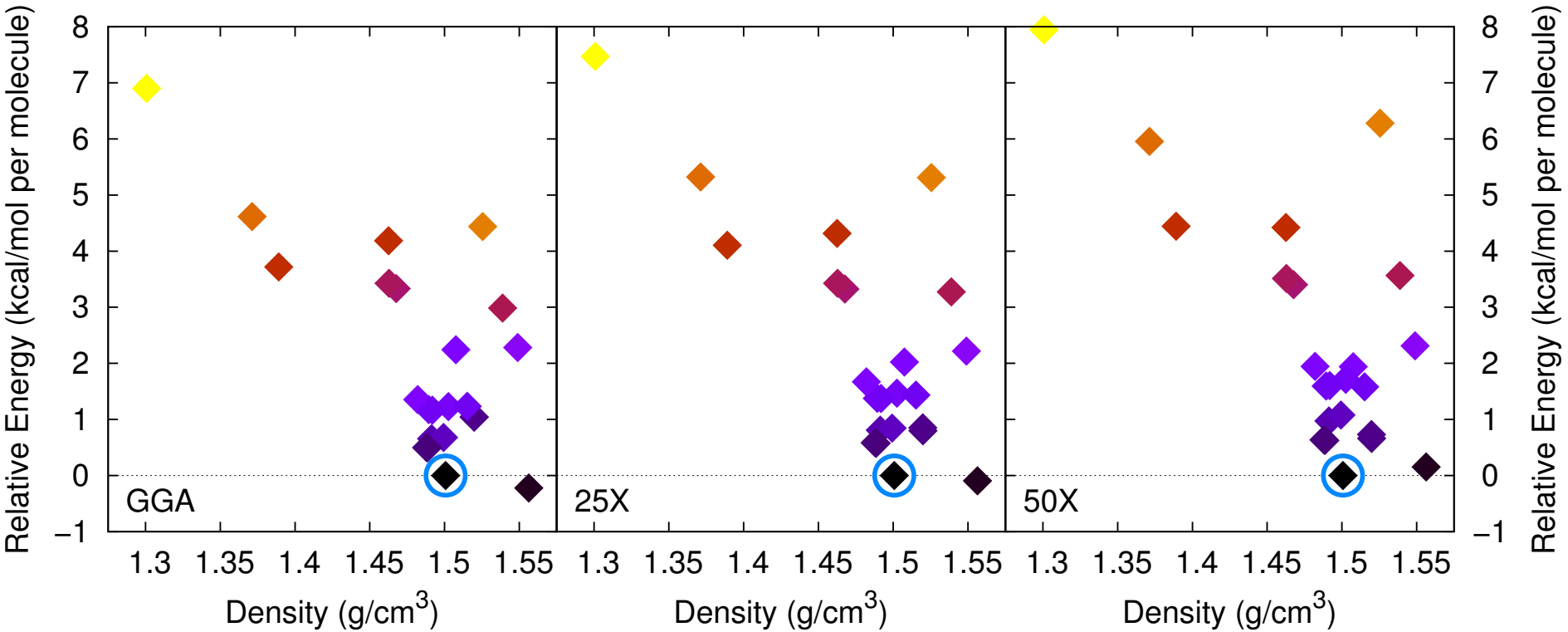

Compound XIX from the 5th CSP Blind test

GGAs show fractional charge transfer (0.82 e^-).

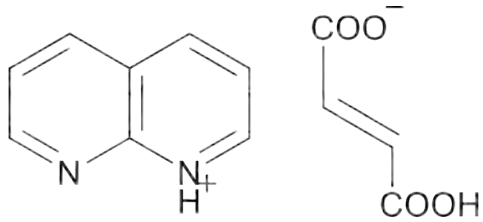

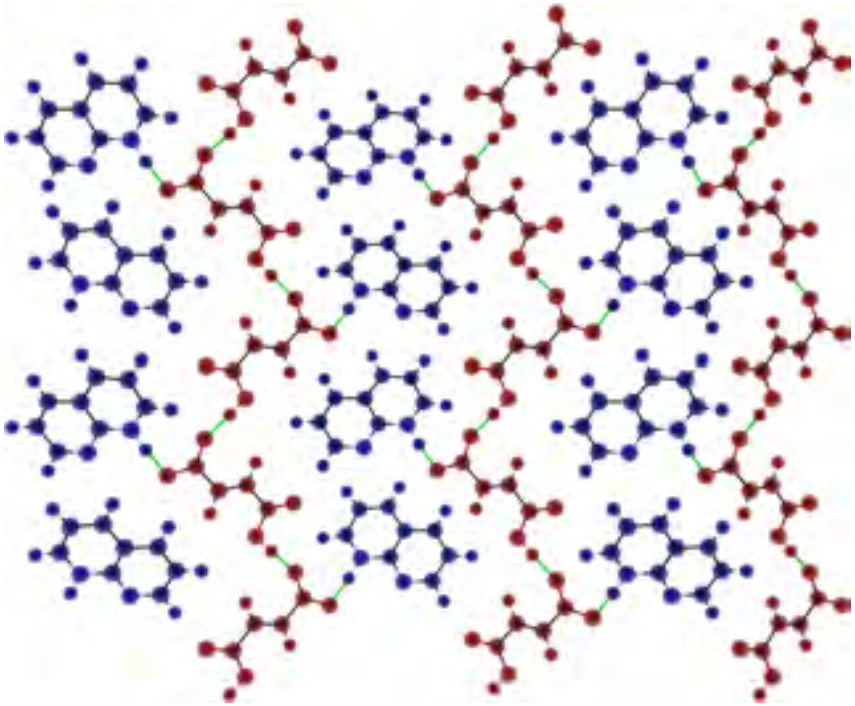

Experimental structure

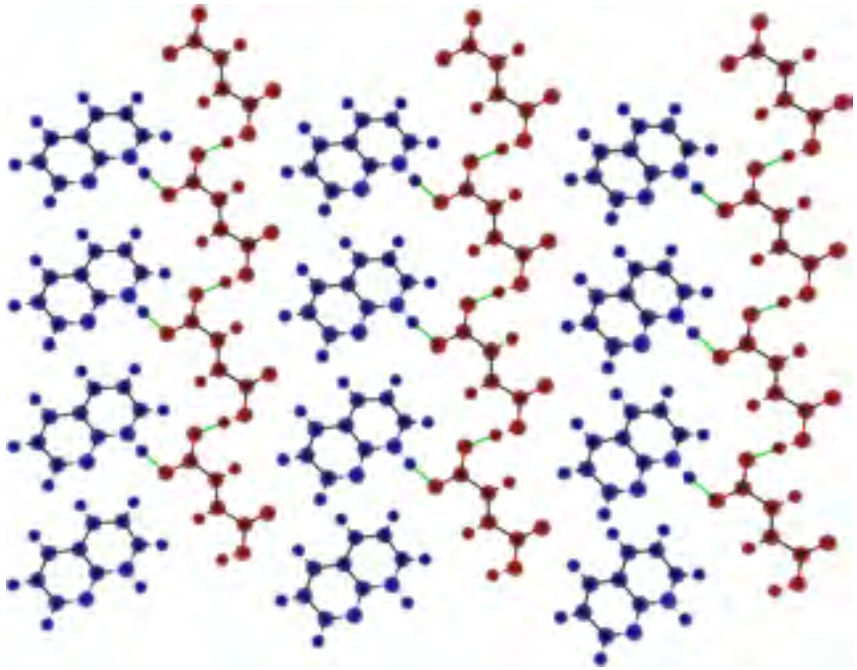

GGA minimum

JCTC **13** (2017) 441

Compound XIX from the 5th CSP Blind test

Inclusion of exact exchange reduces delocalization error.

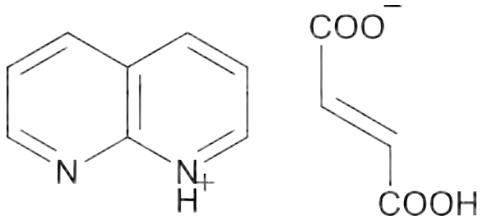

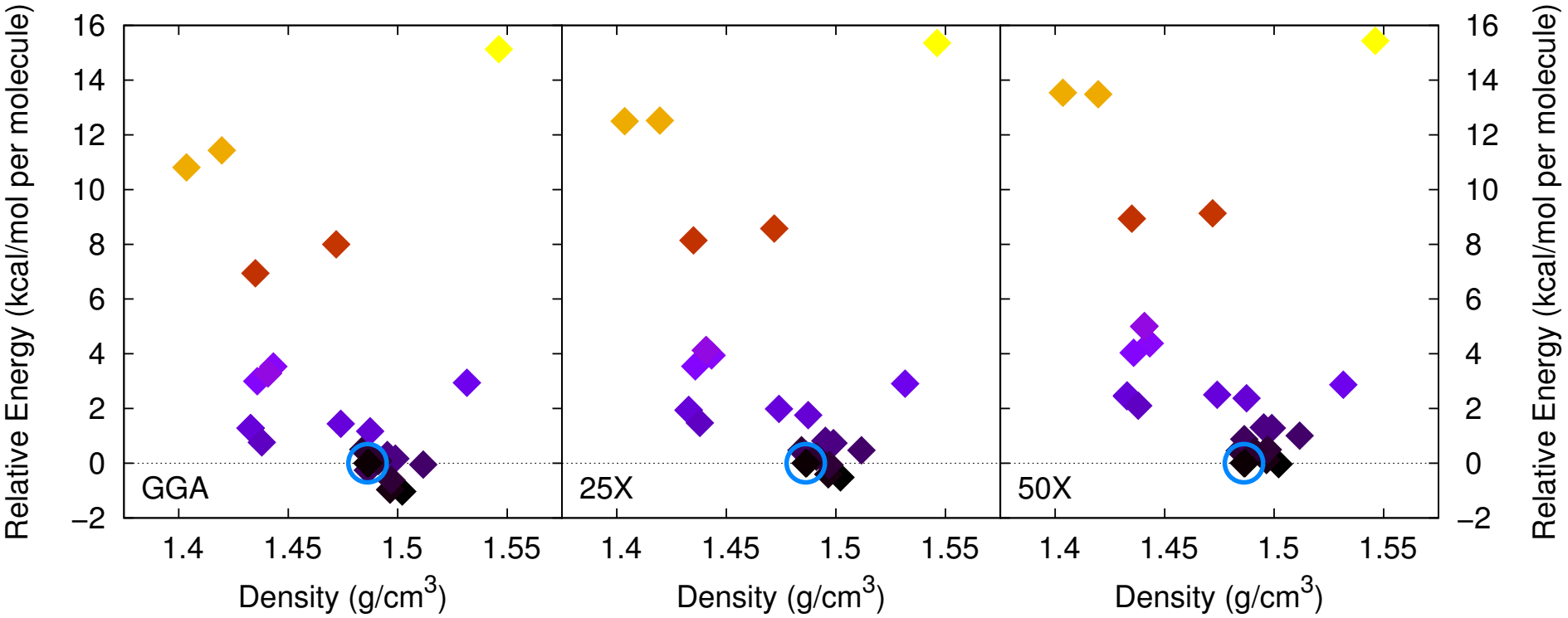

Organic electrides

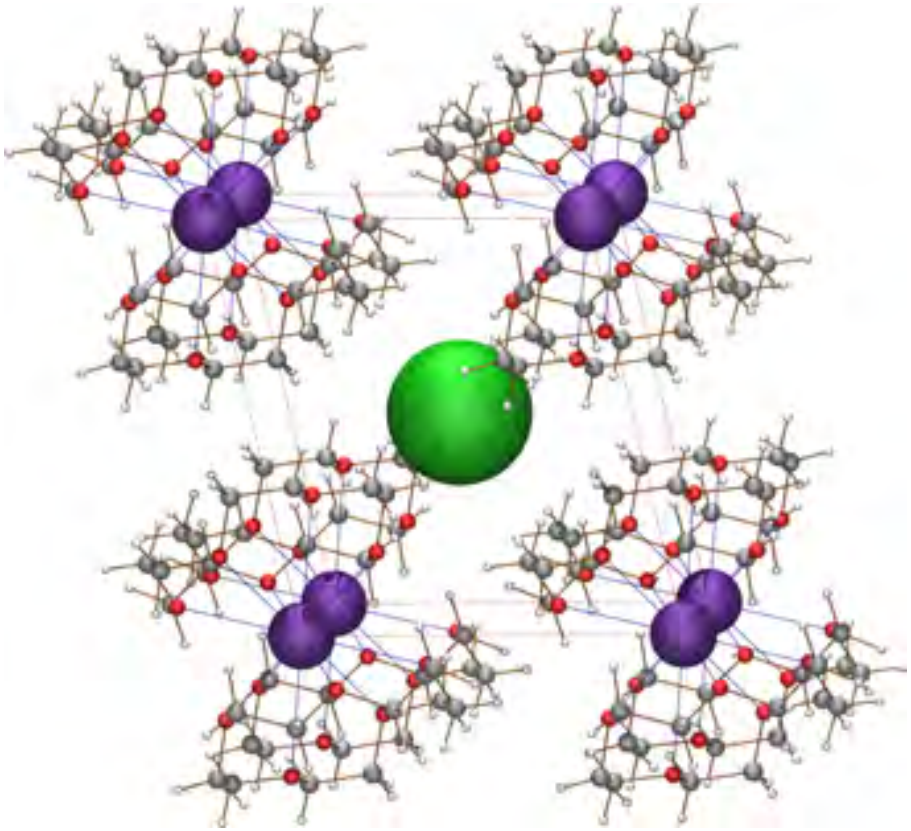

- Ionic materials
- Anions are electrons occupying interstitial voids
- High hyperpolarisabilities
- Extremely low work functions
- Low temperature thermionic emissions
- Very strong reducing character

PCCP **16** (2014) 14584 and **18** (2016) 27326

Band structures

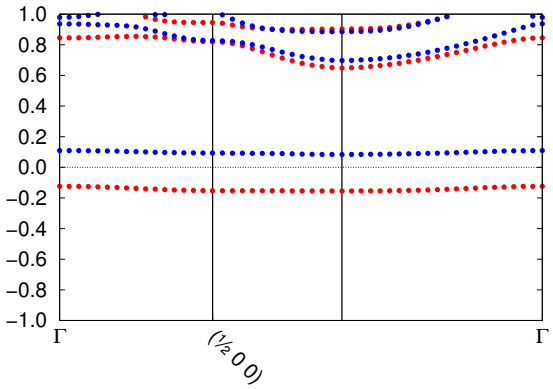

$Cs^+(15C5)_2e^-$

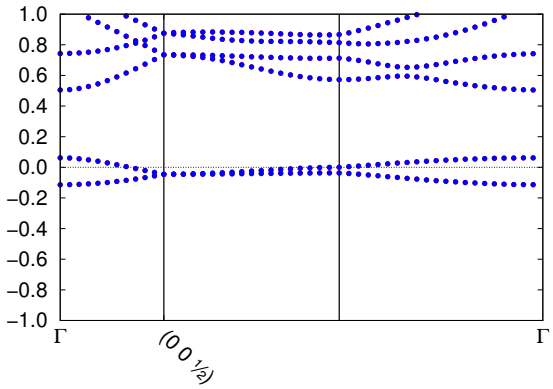

$Cs^+(18C6)_2e^-$

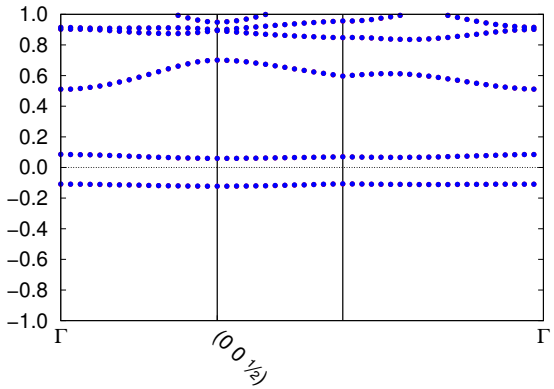

Rb^+(cryptand-2.2.2)e^-

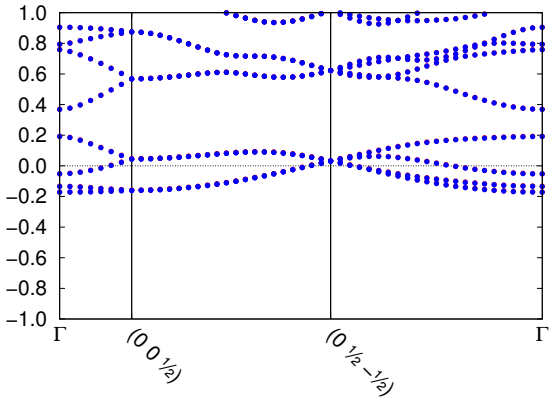

Li^+(cryptand-2.1.1)e^-

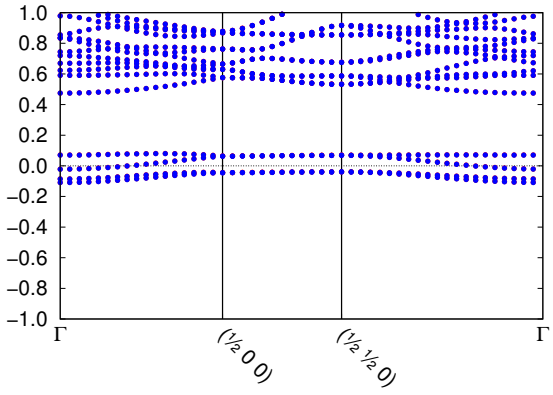

Na^+(tri-pip-aza-2.2.2)e^-

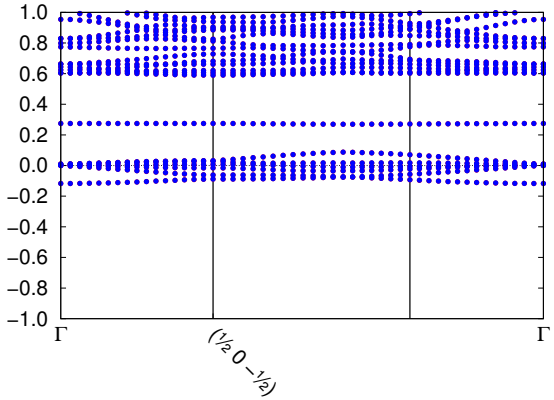

$[Cs^+(15C5)(18C6)e^-]_6(18C6)$

Valence densities

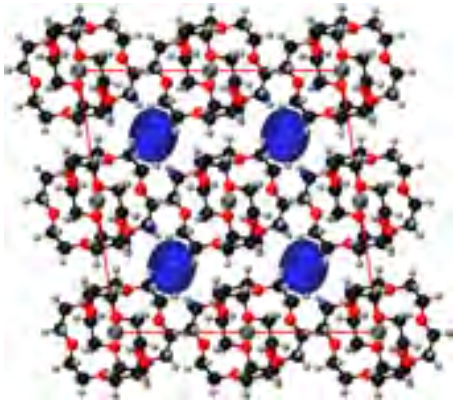

$Cs^+(15C5)_2e^-$

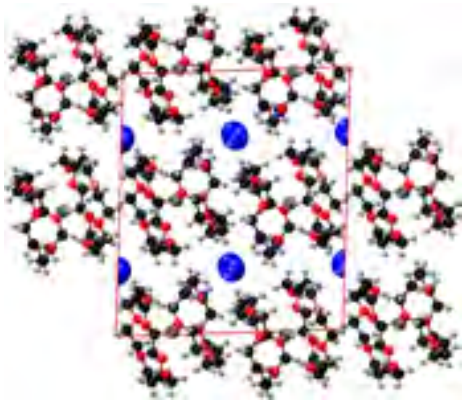

$Cs^+(18C6)_2e^-$

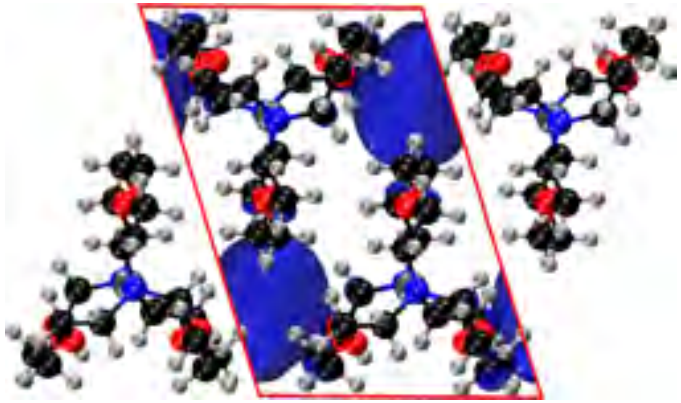

$Rb^+(cryptand\text{-}2.2.2)e^-$

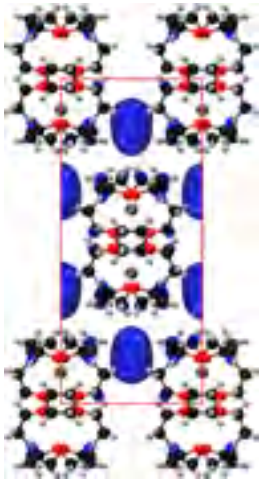

$Li^+(cryptand\text{-}2.1.1)e^-$

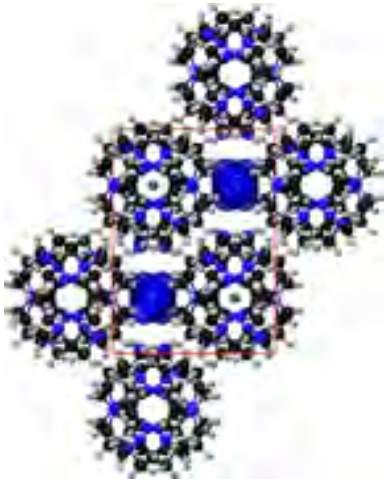

$Na^+(tri\text{-}pip\text{-}aza\text{-}2.2.2)e^-$

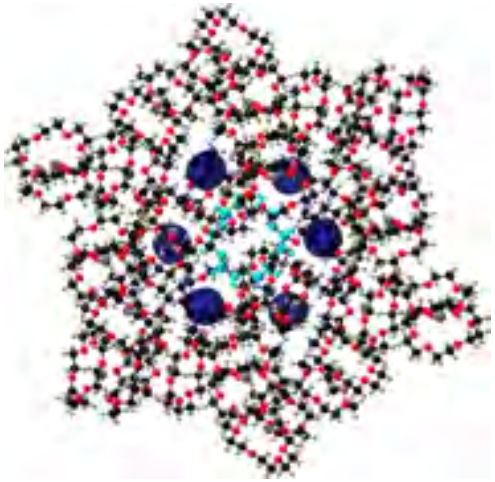

$[Cs^+(15C5)(18C6)e^-]_6(18C6)$

Spin polarisation: antiferromagnetic states

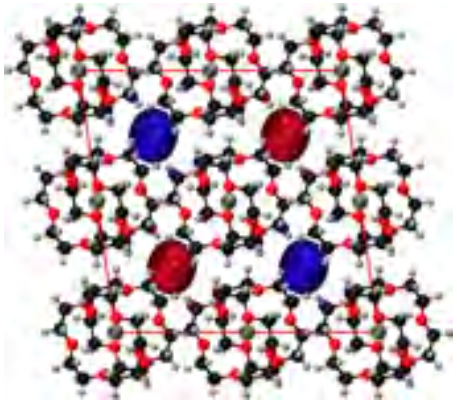

$Cs^+(15C5)_2e^-$

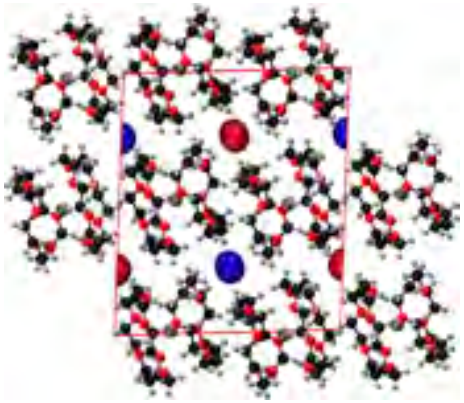

$Cs^+(18C6)_2e^-$

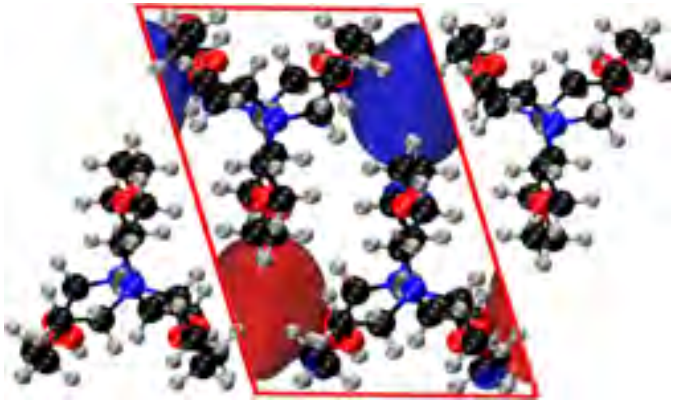

$Rb^+(cryptand\text{-}2.2.2)e^-$

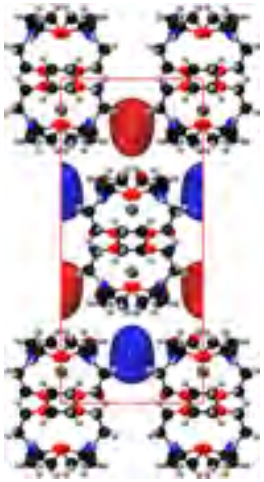

$Li^+(cryptand\text{-}2.1.1)e^-$

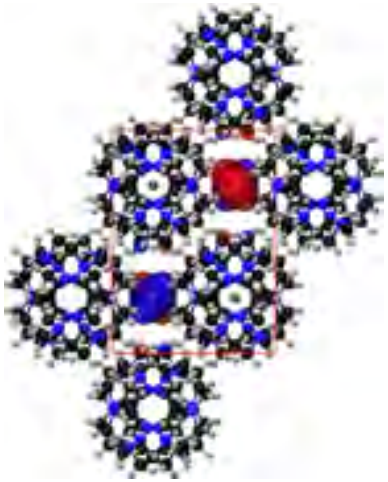

$Na^+(tri\text{-}pip\text{-}aza\text{-}2.2.2)e^-$

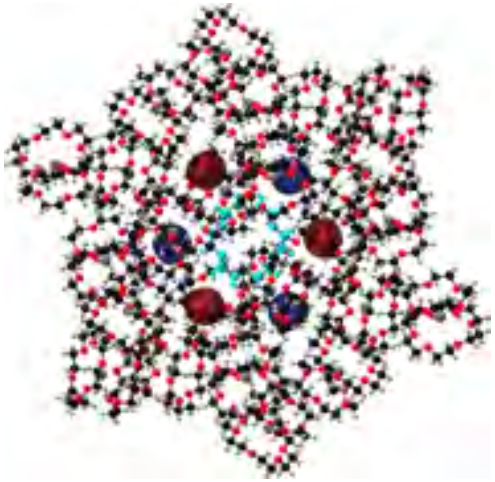

$[Cs^+(15C5)(18C6)e^-]_6(18C6)$

Antiferromagnetic-ferromagnetic transition

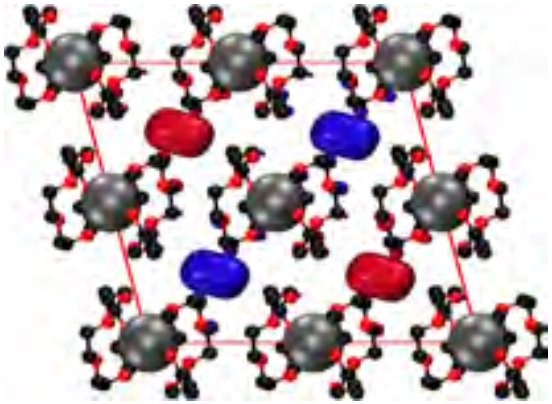

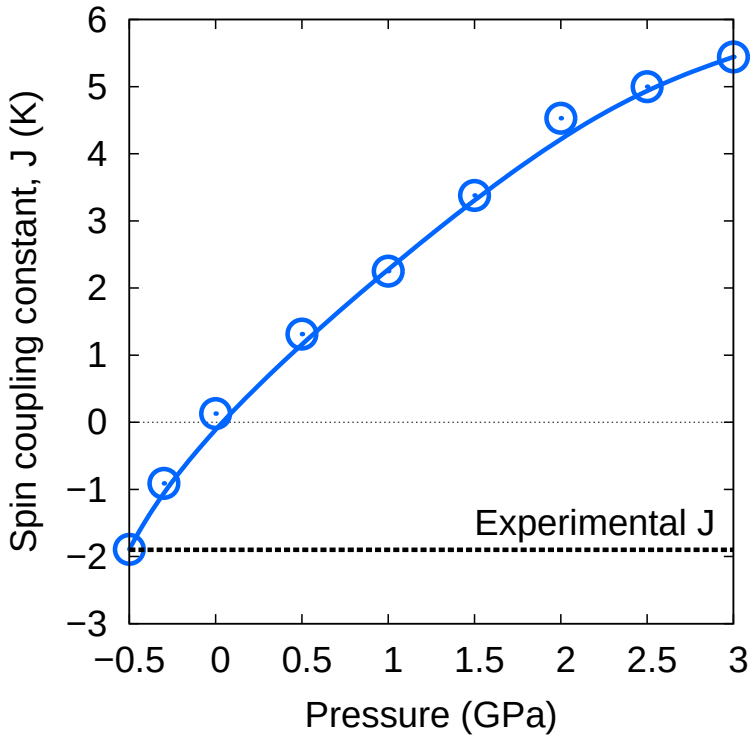

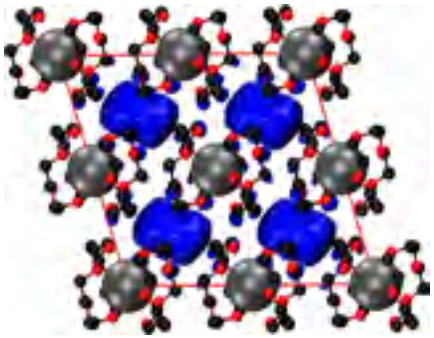

Electrides have the potential to be piezomagnetic materials.

Inorganic electrides

Inorganic electrides are ionic materials where the anions can occupy 0D, 1D, or 2D interstitial voids.

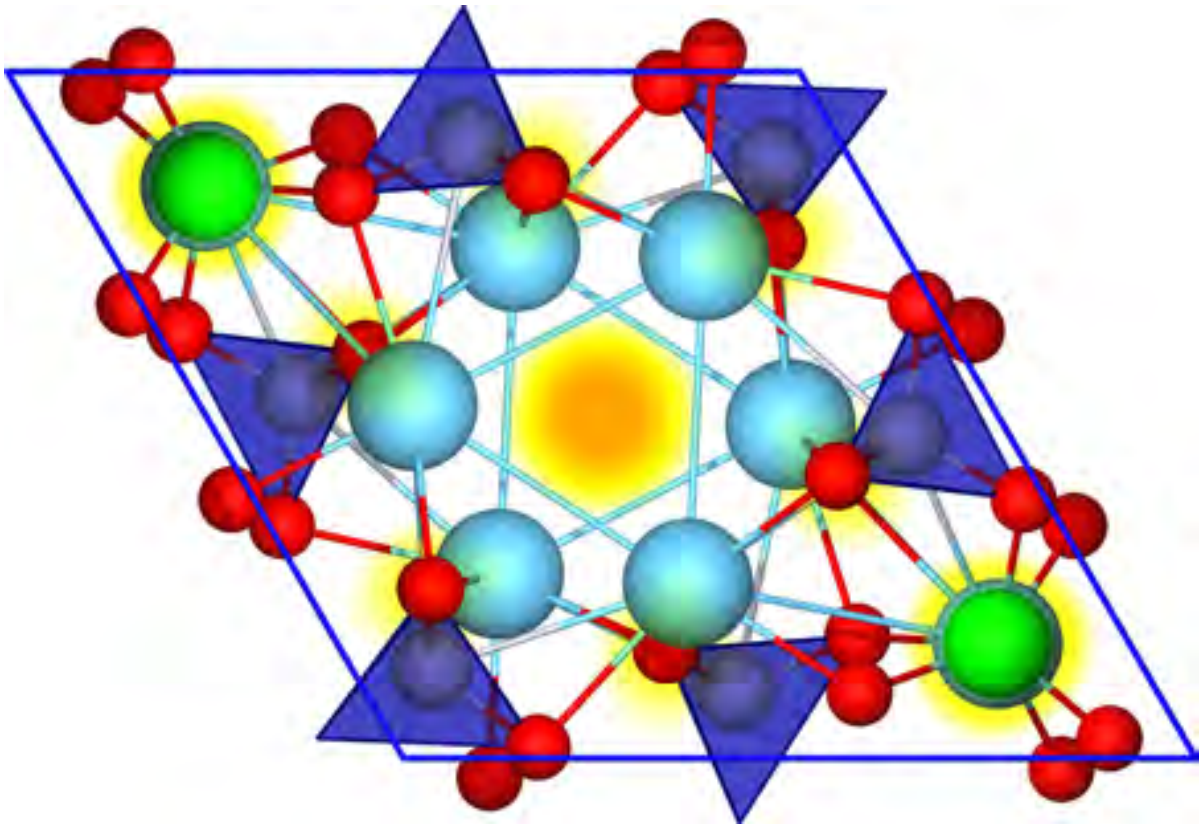

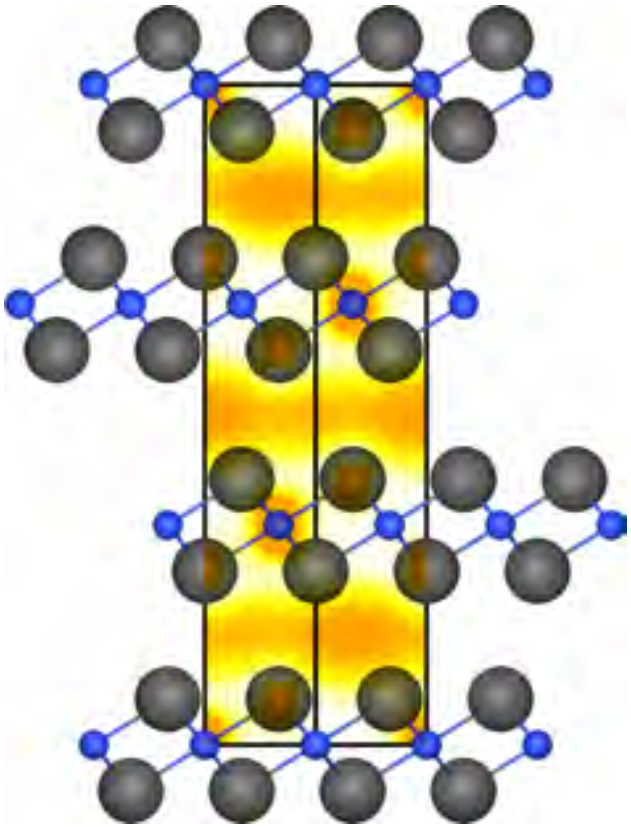

JPCA **122** (2018) 9371

Exfoliation of the layered Ca_2N electride

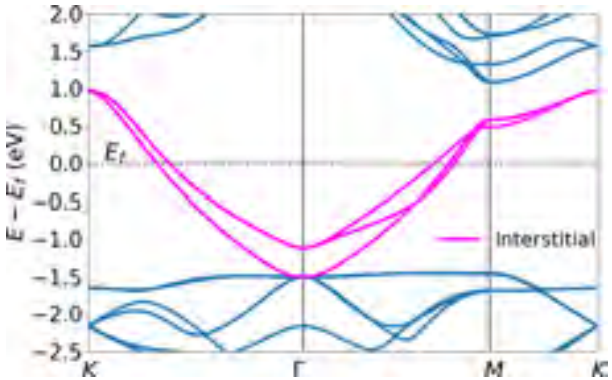

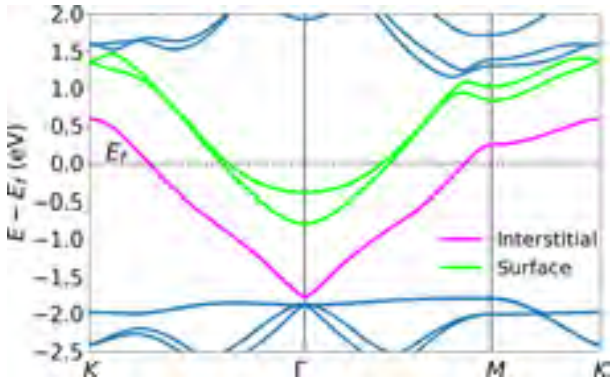

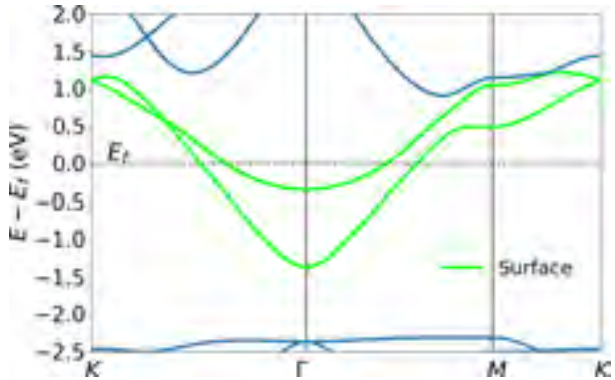

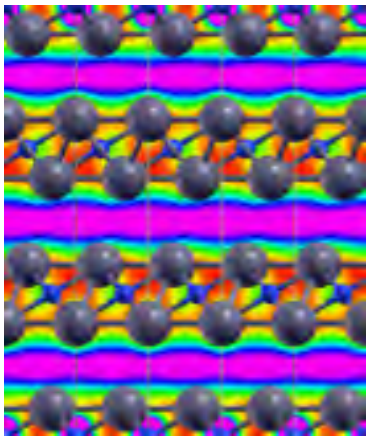

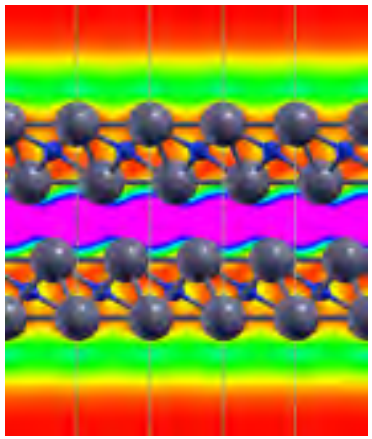

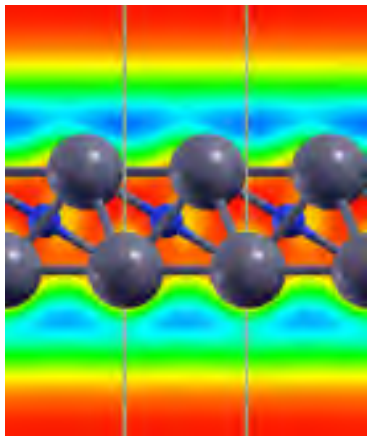

JPCC **125** (2021) 11656

Insertion at an Au-MoS_2 contact

Charge transport from metals to 2D semiconductors, such as MoS_2, is difficult as they form vdW contacts.

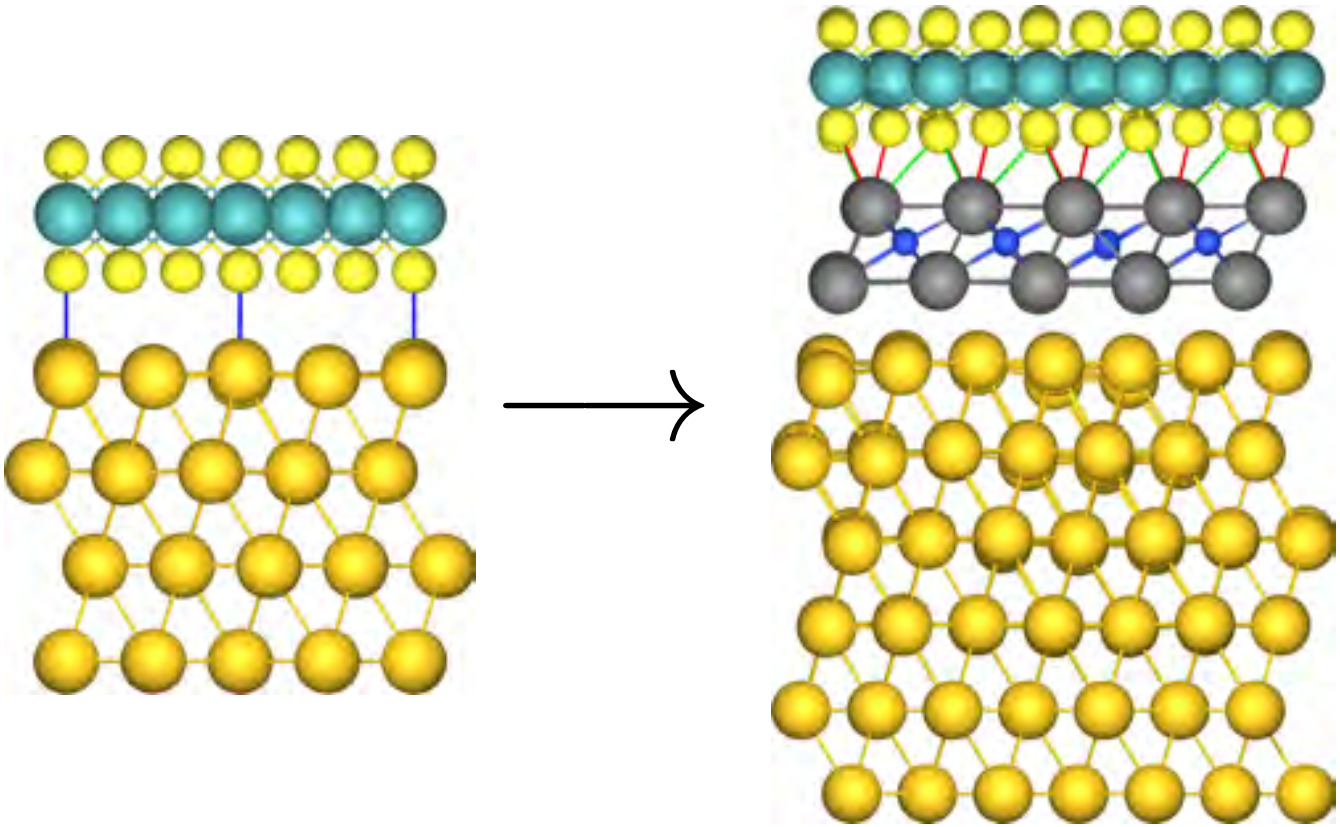

2D electride insertion may facilitate charge transport by doping MoS_2.

Insertion at an Au-MoS_2 contact

The Ca_2N electride dopes the MoS_2, pulling down the conduction band to below the Fermi level.

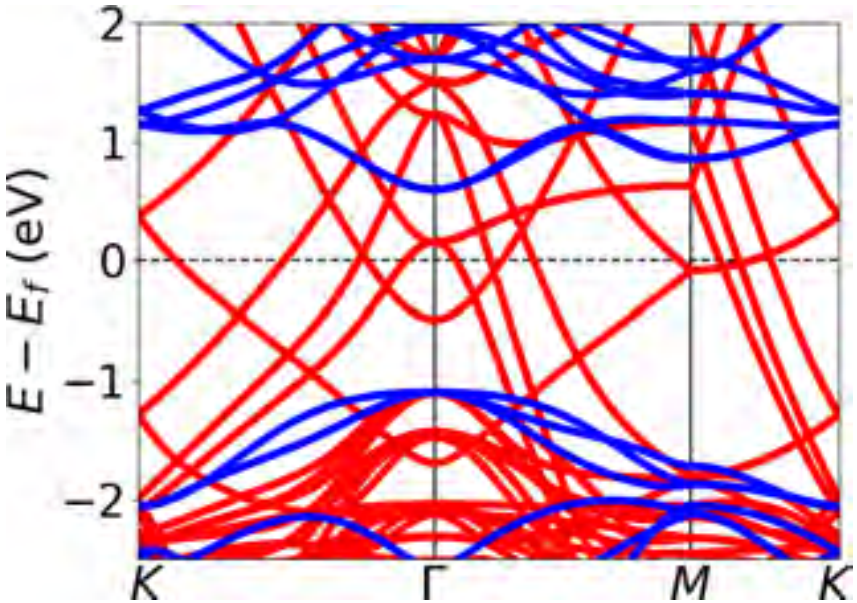

Isolated **Au** and **MoS_2**

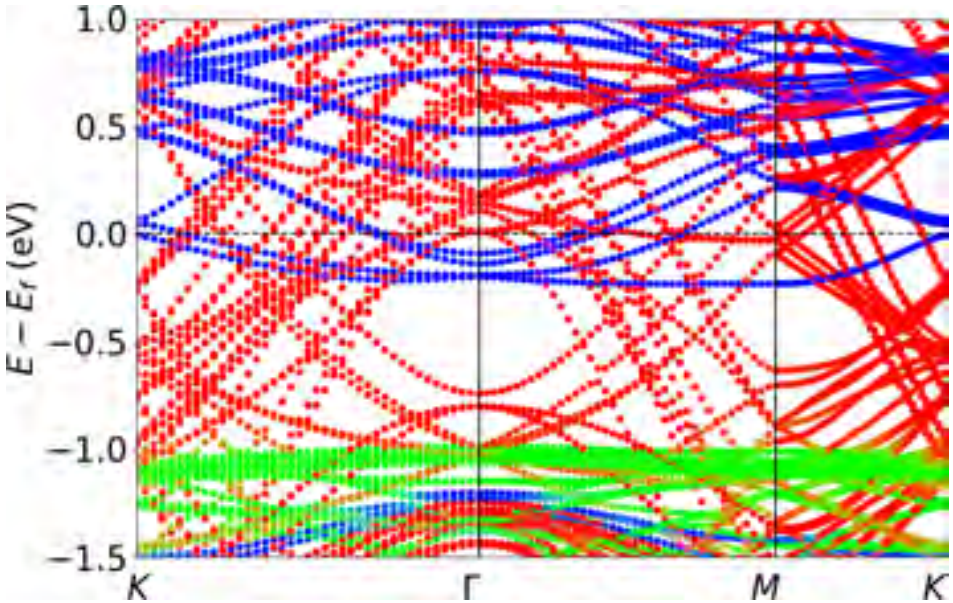

The **Au**–**Ca_2N**–**MoS_2** interface

JPCC **125** (2021) 11656

Insertion at an Au-MoS_2 contact

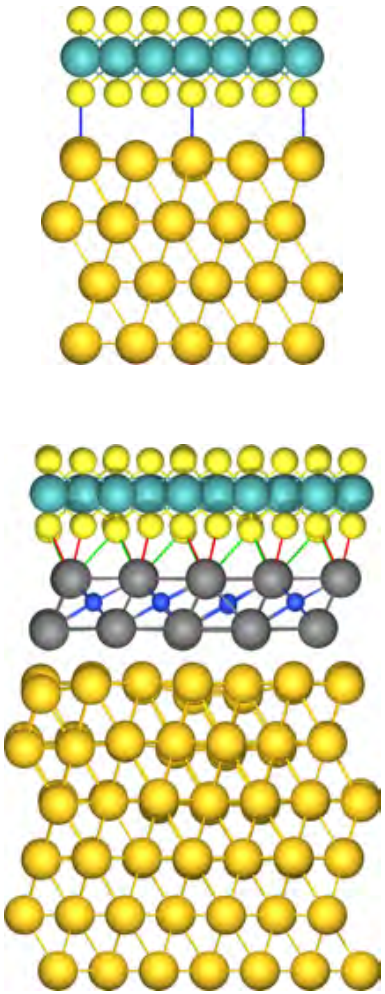

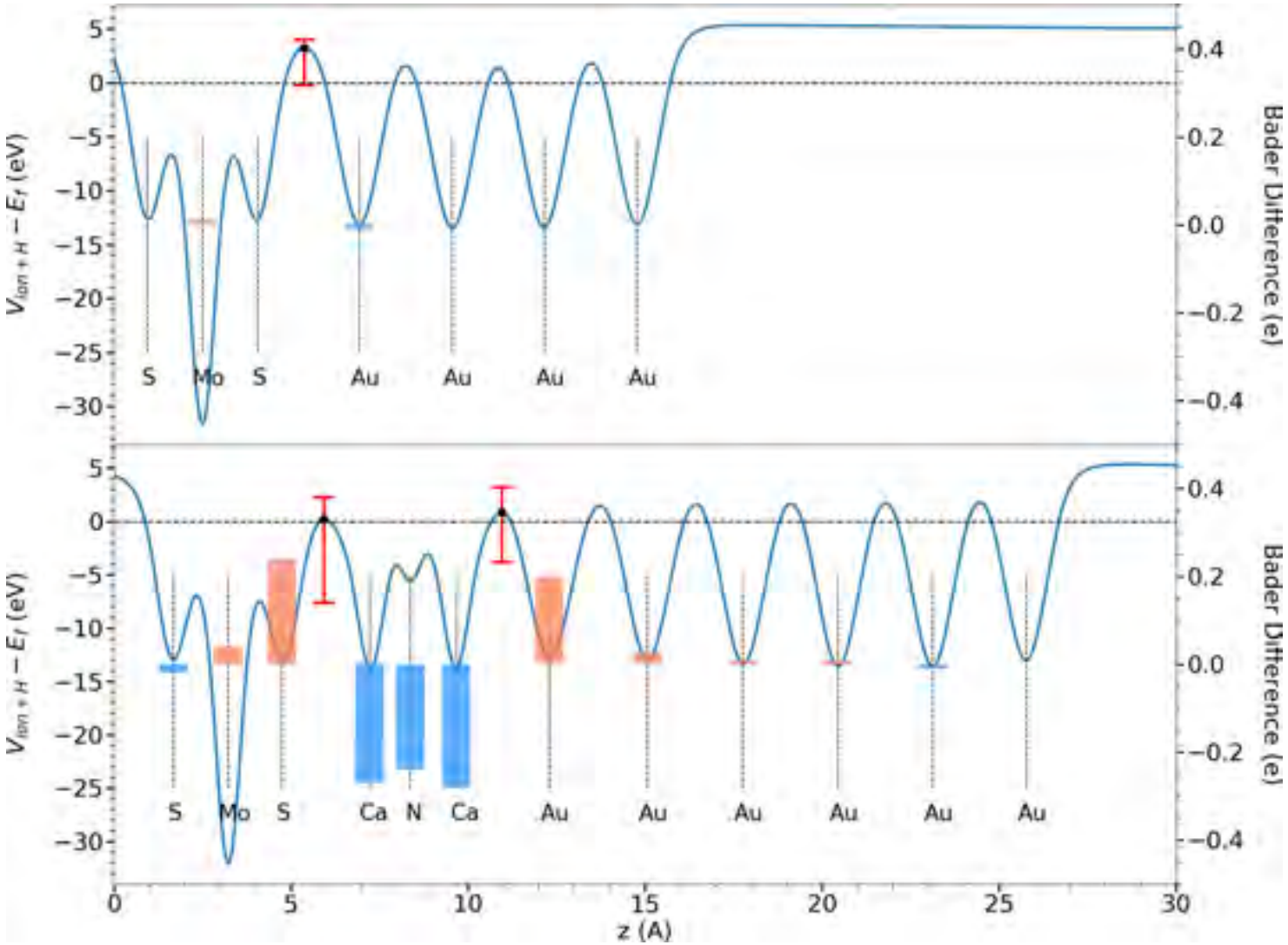

JPCC **125** (2021) 11656

Summary

- XDM is a highly accurate dispersion correction thanks to inclusion of C_8 and C_{10} terms and environment dependence of the dispersion coefficients.
- DFT-XDM is promising for first-principles molecular crystal structure prediction.
- Implementation of XDM in FHI-aims enables higher accuracy and calculations on larger systems than is feasible with plane waves.
- Insertion of 2D electrides at metal-TMDC interfaces may aid charge transport in semi-conductor devices.

Acknowledgements

Current group members:

- **Alastair Price**
- Kyle Bryenton
- Alex Mayo
- Nick Roberts
- Sarah Clarke
- Adrian Rumson
- Adebayo Adeleke
- Cameron Nickerson

Group alumni:

- **Joseph Weatherby**
- Grace Sparrow
- **Fouad Kaadou**
- Sam Dudra (PhD Toronto)
- Tilas Kabengele (PhD Brown)
- Feng “Fred” Xibo (Elsevier)
- **Luc LeBlanc** (PDF Curtin)
- **Matthew Christian** (Sandia)
- **Stephen Dale** (PDF Griffith)
- Joel Mallory (PDF Florida State)
- **Alberto Otero-de-la-Roza** (Oviedo)
- **Sarah Whittleton** (Regeneron Pharma)

Collaborators:

- Axel Becke
- Jesse Maassen
- Kim Jelfs
- Jenny Nelson